



## TREATISE ON GEOPHYSICS - CONTRIBUTORS' INSTRUCTIONS

### PROOFREADING

The text content for your contribution is in final form when you receive proofs. Please read proofs for accuracy and clarity, as well as for typographical errors, but please DO NOT REWRITE.

At the beginning of your article there is a page containing any author queries, keywords, and the authors' full address details.

Please address author queries as necessary. While it is appreciated that some articles will require updating/revising, please try to keep any alterations to a minimum. Excessive alterations may be charged to the contributors.

The shorter version of the address at the beginning of the article will appear under your author/co-author name(s) in the published work and also in a List of Contributors. The longer version shows full contact details and will be used to keep our internal records up-to-date (they will not appear in the published work). For the lead author, this is the address that the honorarium and any offprints will be sent to. Please check that these addresses are correct.

Titles and headings should be checked carefully for spelling and capitalization. Please be sure that the correct typeface and size have been used to indicate the proper level of heading. Review numbered items for proper order – e.g., tables, figures, footnotes, and lists. Proofread the captions and credit lines of illustrations and tables. Ensure that any material requiring permissions has the required credit line, and that the corresponding documentation has been sent to Elsevier.

Note that these proofs may not resemble the image quality of the final printed version of the work, and are for content checking only. Artwork will have been redrawn/relabelled as necessary, and is represented at the final size.

PLEASE KEEP A COPY OF ANY CORRECTIONS YOU MAKE.

### DISPATCH OF CORRECTIONS

Proof corrections should be returned in one communication to your academic editor **Dr Adam Dziewonski** by **12-04-2007** using one of the following methods:

1. If corrections are minor they should be listed in an e-mail to [dziewons@seismology.harvard.edu](mailto:dziewons@seismology.harvard.edu). A copy should also be sent to: [TOGPproofs@elsevier.com](mailto:TOGPproofs@elsevier.com). The e-mail should state the article code number in the subject line. Corrections should be consecutively numbered and should state the paragraph number, line number within that paragraph, and the correction.

2. If corrections are substantial, send the amended hardcopy by courier to **Dr Adam Dziewonski, Department of Geological Sciences, Harvard University, 20, Oxford Street, Cambridge, MA 02138, USA**, with a copy by fax to the Elsevier MRW Production Department (fax number: +44 (0)1865 843974). If it is not possible to courier your corrections, fax the relevant marked pages to the Elsevier MRW Production Department with a covering note clearly stating the article code number and title.

Note that a delay in the return of proofs could mean a delay in publication. Should we not receive your corrected proofs within 7 days, Elsevier may have to proceed without your corrections.

### CHECKLIST

- |   |                          |
|---|--------------------------|
| Author queries addressed/answered?                      | <input type="checkbox"/> |
| Affiliations, names and addresses checked and verified? | <input type="checkbox"/> |
| 'Further Reading' section checked and completed?        | <input type="checkbox"/> |
| Permissions details checked and completed?              | <input type="checkbox"/> |
| Outstanding permissions letters attached/enclosed?      | <input type="checkbox"/> |
| Figures and tables checked?                             | <input type="checkbox"/> |

If you have any questions regarding these proofs please contact the Elsevier MRW Production Department at: [TOGPproofs@elsevier.com](mailto:TOGPproofs@elsevier.com).



## TREATISE ON GEOPHYSICS - EDITORS' INSTRUCTIONS

### PROOFREADING

Please find attached PDF proofs for **00001**. A copy of these proofs has been sent to the lead author, along with any manuscript queries. We have asked them to send their corrections to you by **12-04-2007**.

Note that these proofs may not resemble the image quality of the final printed version of the work, and are for content checking only. Artwork will have been redrawn/relabelled as necessary, and is represented at the final size.

Proof corrections from contributors will reach you in one of the following ways:

1. If corrections are minor they will be e-mailed to you by the contributor. This e-mail will state the article code number. Upon receiving this e-mail please amend/approve contributor corrections (if necessary) and add your corrections (if any) to the e-mail and forward it to the Elsevier MRW Production Department at: [TOGPproofs@elsevier.com](mailto:TOGPproofs@elsevier.com).
2. If corrections are more substantial, the amended hardcopy will be sent directly to you by courier (or from the contributor to Elsevier by fax and then forwarded to you as an e-mail). Please add your corrections to a hardcopy and fax any amended pages to the Elsevier MRW Production Department on +44 (0)1865 843974, with a cover note stating the article code number and title.

PLEASE KEEP A COPY OF ANY CORRECTIONS.

Please note the following points:

#### Title

Check that article titles are appropriate, and inform us of any proposed changes.

#### Spelling

If you notice any spelling errors, please point them out to us. You should have a copy of the current world and abbreviation lists.

#### Cross-references

**Please ensure that all cross-references to other articles are in place - if there are none present, please insert as necessary.** 'See' references should appear within the main article text and will link directly with relevant articles. 'See also' references will appear at the end of each article, and will link to useful related (but not necessarily directly related) articles. PLEASE USE MANUSCRIPT CODE NUMBERS RATHER THAN INDIVIDUAL TITLES. Along with the first batch of proofs, you will receive an up-to-date article list showing article titles and code numbers.

#### Further Reading

Check all titles are present, and listed in the correct format. This section should not exceed 15 titles.

Look through the proofs and add your comments. Once you have received and approved the contributors' corrections, collate them with yours. Please try to keep any alterations to a minimum.

### DISPATCH OF CORRECTIONS

Please send corrections for these proofs to the Elsevier MRW Production Department by **23-04-2007** at the latest. You should forward your comments to us within this time even if the relevant contributors have not sent their corrections to you.

PLEASE KEEP A RECORD OF WHICH ARTICLES YOU HAVE RECEIVED AND WHEN, IN ADDITION TO THE DATE YOU RETURNED COLLATED PROOFS TO US.

If you have any questions regarding these proofs please contact the Elsevier MRW Production Department at: [TOGPproofs@elsevier.com](mailto:TOGPproofs@elsevier.com).

## Author Query Form

---

Comprehensive Treatise on Geophysics

Article: 00001

Dear Author,

Please respond to the queries listed below. You may write your comments on this page, but please write clearly as illegible mark-ups may delay publication. If returning the proof by fax do not write too close to the paper's edge.

Please note that these queries have been raised by Elsevier's appointed copy-editors, and not by your academic editor.

Thank you for your assistance.

### AUTHOR QUERIES

---

AU1 Please check the long affiliations for accuracy. These are for Elsevier's records and will not appear in the printed work.

---

AU2 Please provide keywords and abstract for this chapter.

---

AU3 "Oldham (1906)" is not listed in "References" section. Please check.

---

AU4 "Bullen (1939) is not listed in "References" section. Please check.

---

AU5 Bullen (1949) is not listed in "References" section. Please check.

---

AU6 Benioff (1958) is not listed in "References" section. Please check.

---

AU7 Johnson, 1966 is not listed in "References" section. Please check.

---

AU8 Birch, 1952 is not listed in "References" section. Please check.

---

- 
- AU9 Brune and Dorman (1963) is not listed in “References” section. Please check.
- 
- AU10 Hart and Anderson (1978) is not listed in “References” section. Please check.
- 
- AU11 Ekström and Dziewonski, 1998 is not listed in “References” section. Please check.
- 
- AU12 Buland *et al.*, 1979, 1998 is not listed in “References” section. Please check.
- 
- AU13 Woodhouse and Girnius (1982) is not listed in “References” section. Please check.
- 
- AU14 Dziewonski and Steim, 1982 is not listed in “References” section. Please check.
- 
- AU15 Woodward and Masters (1991) is not listed in “References” section. Please check.
- 
- AU16 Kustowski *et al.* (2006) is not listed in “References” section. Please check.
- 
- AU17 Gung and Romanowicz, 2004 is not listed in “References” section. Please check.
- 
- AU18 Dziewonski *et al.*, 2006 is not listed in “References” section. Please check.
- 
- AU19 Yoshizawa and Kennett (2002) is not listed in “References” section. Please check.
- 
- AU20 Please supply first 3 author names in place of *et al.* if number of authors are more than 6; otherwise, supply all the author names.
- 
- AU21 Do Figures 1–23 require permission? If yes, please provide the permission letters granting permission and the complete source details, wherever not provided.
- 
- AU22 Please check if “5 Hz to 360 seconds” is correct.
-

---

AU23 Wielandt (2002) is not listed in “References” section. Please check.

---

AU24 Anderson (1963) is not listed in “References” section. Please check.

---

AU25 Stein and Wyssession (2003) is not listed in “References” section. Please check.

---

AU26 Please provide high resolution figures for figure 13, 18 and 22.

---

ELSEVIER FIRST PROOF

a0005

## 1.01 Overview

**A. M. Dziewonski**, Harvard University, Cambridge, MA, USA

**B. A. Romanowicz**, University of California at Berkeley, Berkeley, CA, USA

© 2007 Elsevier Ltd. All rights reserved.

1.01.1	Developments from the Late Nineteenth Century until the Early 1950s	2
1.01.2	Developments from 1950s through the Early 1980s	5
1.01.3	From 1980 to Present: The Era of Tomography and Broadband Digital Seismic Networks	11
1.01.4	Current Issues in Global Tomography	17
References		25

**AU2** p0005 Applications of seismology to the study of the Earth's interior are only about 100 years old. Its tools in determining the properties of inaccessible Earth are the most powerful among all geophysical methods. The principal reasons are the availability of natural (earthquakes) or controlled (explosions, vibrators) sources of elastic waves and their relatively low attenuation with distance. Seismological methods span some six orders of magnitude in frequency and the depth of an investigated structure may range from a few meters in engineering applications to the center of the Earth. Progress in seismology has been achieved through developments on several fronts: theory, instrumentation and its deployment, as well as computational resources.

p0010 Even though the studies of earthquakes and Earth's structure are closely related, the two subjects are often discussed separately. This volume is devoted to the Earth's structure, and Volume 4 to studies of earthquakes. Nevertheless, the relationship is intimate. For example, it is possible to formulate an inverse problem in which earthquake locations are sought simultaneously with the parameters of the Earth's structure, including three-dimensional (3-D) models (*see* 00009).

p0015 In the last 25 years, important progress has been made on several fronts: (1) the development of broadband digital instrumentation, which has allowed the construction of digital seismic databases of unprecedented quality at both the global and regional scales; (2) the development of powerful data analysis tools, made possible by ever more computer technology; and (3) theoretical progress in the forward and inverse computation of the effects of strong lateral heterogeneity on seismic-wave propagation. The combination of these factors has led to much improved images of

structure at the global and regional scale, often helped by the inclusion of constraints from other types of data, primarily from the fields of mineral physics and geodynamics. This volume is thus divided into four parts. The first part principally covers theoretical developments and seismic data analysis techniques. 00002 discusses the state of the art in the computation of the Earth's normal modes, while 00003 describes progress in the measurements of normal-mode and long-period surface waves. Two chapters are devoted to the computation of synthetic seismograms in the presence of lateral heterogeneity, suitable for the case of body waves (*see* 00004, 00005). Significant progress has recently been made in the computation of synthetic seismograms in a 3-D Earth using numerical methods. A review is given in 00006. With the deployment of dense regional arrays of broadband seismometers, another area of rapid progress has been that of the adaptation of methodologies first developed in exploration seismology to the case of fine structure imaging of the crust and upper mantle at larger scale. These approaches are described in 00008 for passive-source applications, and in 00014, for the case of active sources. The realization of the importance of anisotropy in the Earth has led to theoretical and methodological developments (*see* 00007). Note that the issue of anisotropy is also discussed in 00018 in the context of inversion of surface-wave data. Inverse methods, in particular in the context of global and regional tomography, are discussed in 00009.

In the second part of Volume 1, reviews of the **p0020** status of our knowledge on the structure of the Earth's shallow layers are presented, starting with a global review of the Earth's crustal structure (*see* 00011). Two chapters discuss regional structure in

## 2 Overview

the oceans: 00012 for mid-ocean ridges and 00013 for hot-spot swells. Finally, two chapters are devoted to the results of regional experiments: upper-mantle studies using data from portable broadband experiments (*see* 00015) and crustal studies, specifically in Europe, from high-resolution long-range active-source experiments (*see* 00016).

p0025 The third part of this volume concerns the Earth's deep structure, divided into its main units: the upper mantle (00018), the transition zone and upper-mantle discontinuities (00020), the D'' region at the base of the mantle (00022) as well as the Earth's core (00023). 00021 is devoted to the subject of scattering in the Earth and 00024 to that of attenuation. Finally, the third part of this volume comprises two chapters, in which constraints on Earth structure from fields other than seismology: mineral physics (*see* 00026) as well as geodynamics (*see* 00027) are discussed.

p0030 This volume addresses various aspects of 'structural seismology' and its applications to other fields of Earth sciences. Not all the subjects are covered in comparable detail, even though the completeness of the coverage was the initial objective of the editors. In particular, there is no chapter on instrumentation, and we have tried to partially make up for it by discussing this subject in this overview; portable instrumentation is discussed to some extent in the 00015. We also present our point of view on current issues in global tomography not discussed in any of the chapters.

p0035 We thus proceed to describe briefly the developments in seismology from the end of the nineteenth century until the present, with the main emphasis on the development of instrumentation and its deployment, because seismology is a data-driven science. An account of the history of seismology can be found, among others, in Agnew (2002).

### s0005 1.01.1 Developments from the Late Nineteenth Century until the Early 1950s

p0040 The theoretical beginnings of seismology may be traced to the eighteenth and nineteenth century studies of elasticity and propagation of elastic waves in solids. Lord Kelvin provided the first numerical estimate of the period of the fundamental vibrational mode ( ${}_0S_2$ ) in 1863, but the development of the proper theory for a homogeneous sphere had to wait nearly 50 years (Love, 1911). Lord Rayleigh solved the problem of propagation of surface waves in an elastic half-space in 1877.

This preceded the first mechanical seismographs, p0045 which were developed in the 1880s. Originally, the seismographs had very low sensitivity and were used for the recording of local earthquakes. The history of global seismology begins with the recording of an earthquake in Japan on 19 April, 1889 by von Rebeur-Paschwitz. He associated a disturbance recorded on a tiltmeter, used to study the Earth's tides, with the reports of a great earthquake in Japan. **Figure 1** shows a copy of this recording as published in *Nature* (1889).

The early seismographs were mechanical pendu- p0050 lums with no damping, other than friction. Their magnifications (the ratio of the amplitude on a seismogram to the actual ground motion) were very low, and because of the lack of damping, the records were very oscillatory and it was difficult to distinguish the arrivals of different phases. An improved mechanical seismograph with controlled damping<sup>b0100</sup> was built by Wiechert in 1904. Soon afterward Galitzin (1914) developed an electromagnetic seismograph system, where the motion of the seismometer's pendulum generated an electric current by motion of a coil in the magnetic field. This current was, in turn, carried to a galvanometer; the rotation of the galvanometer's coil in a magnetic field was recorded on photographic paper by a beam of light reflected from a mirror attached to the coil. The response of the system depended on the sensitivity and free period of the seismometer and of the galvanometer and their damping. While the system was more complex, it allowed

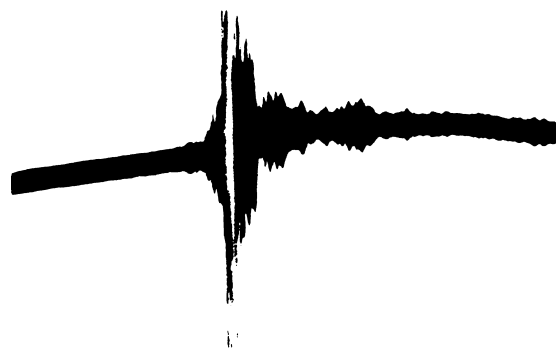


**Figure 1** The historical first recording of a teleseismic event: an earthquake in Japan recorded in Potsdam on a tiltmeter designed by von Rebeur-Paschwitz. The early seismographs had difficulty with damping the pendulum<sup>b0100</sup> motion and made phase identification difficult. From Agnew DC, *et al.* (2002) *History of seismology*. In: Lee WHK, Kanamori H, Jennings PC, and Kisslinger C (eds.) *International Handbook of Earthquake and Engineering Seismology*, pp. 3–12. San Diego, CA: Academic Press.

f0005  
AU21

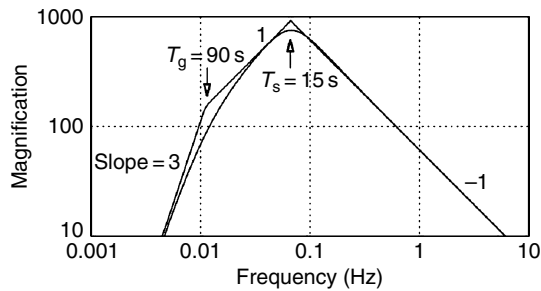


**Figure 2** Plot of the ground-motion (amplitude) response of a WWSSN station with a seismograph free period ( $T_s$ ) of 15 s and galvanometer with a free period ( $T_g$ ) of 90 s. The segment between these two periods has a flat velocity response, characteristic of broadband seismometers. The response in modern instruments is shaped electronically; a typical FDSN station has a flat velocity response from 5 Hz to 360 seconds. From Wielandt (2002).

for much more flexibility in selecting a desired response. **Figure 2** shows the response of the seismograph–galvanometer system and gives an idea of the way it could be shaped by the choice of different free periods of the system’s components. With gradual improvements, the seismometer–galvanometer system and recording on photographic paper was commonly used during the following 60–70 years, when it was gradually replaced by digital systems.

With the improvement of the recording systems technology, phase identification became easier, and it was possible to identify P-arrivals (primary) corresponding to compressional waves, S-arrivals (secondary) corresponding to shear waves, and L-arrivals, sometimes called ‘the main phase’, corresponding to surface waves. The surface waves caused some confusion because there was also a transverse motion, not predicted by Rayleigh. It was not until 1911 that Love showed that transversely polarized surface waves can propagate in a layered Earth.

Progress in the first decade of the twentieth century was rapid. Some classical problems such as computation and inversion of traveltimes for the velocity structure were solved by Benndorf (1905, 1906), Herglotz (1907), and Wiechert (1907); Knott (1899) and Zöppritz (1907) independently developed equations for the amplitude of reflected and transmitted waves at the boundary between two elastic media.

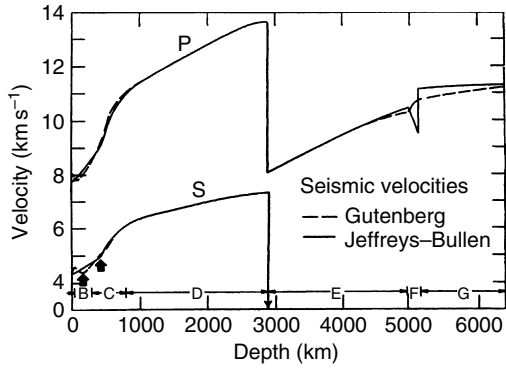
As regards Earth’s structure, there was a paper by Oldham (1906), in which he proposed the existence of the Earth’s core, although there has been some confusion in identification of phases: what he thought to be a delayed S-wave was actually an SS. Gutenberg (1913) properly identified reflections

from the core–mantle boundary and determined the radius of the core quite accurately, and Jeffreys (1926) showed that the core is liquid. Mohorovičić (1910) discovered the boundary between the crust and upper mantle, thus beginning the era of studies of the crust and lithosphere, which greatly accelerated after World War II.

The first global seismographic networks were established in the early years of the twentieth century. The first one was deployed by John Milne in various countries of the British Commonwealth with the support of the British Association for the Advancement of Science and eventually consisted of 30 stations (Adams, 2002). The Jesuit Network was established soon afterward, with a particularly large number of instruments in the United States, but also including stations on all continents (Udias and Stauder, 2002). With a global coverage sufficient to locate large earthquakes, informal bulletins were published using the location method developed by Geiger (1910, 1912), which (with many modifications) is still used today. In 1922, the International Seismological Summary (ISS), with international governance, was established under Professor Turner of Oxford University with the charge to produce ‘definitive global catalogs’ from 1918 onward.

The slow progress in unraveling the Earth structure culminated in the 1930s with the discovery of the inner core by Inge Lehmann (1936) and the compressional velocity, shear velocity and density models by Gutenberg (1913), Jeffreys (1926), and Bullen (1939). The Gutenberg and Jeffreys velocity models are shown in **Figure 3**; except for the details of the upper-mantle structure, these models are very similar to the modern ones. The low-velocity zone above the inner–outer core boundary in the model of Jeffreys illustrates the sometimes unfortunate tendency of seismologists to introduce physically implausible features in the model in order to match the data; Jeffreys needed to add a 2 s delay to match the inner-core traveltimes and accomplished it by inserting this feature, which is impossible to reconcile with the chemical and physical properties of materials in this depth range. The other important difference between the models of Jeffreys and Gutenberg was the existence of a low-velocity zone in the depth range 100–200 km in the upper mantle. There were very hot debates on this issue; it now can be explained by the fact that they used data from tectonically different regions; there is a low-velocity zone in the Western US, but not under the Eurasian Shield regions.

4 Overview

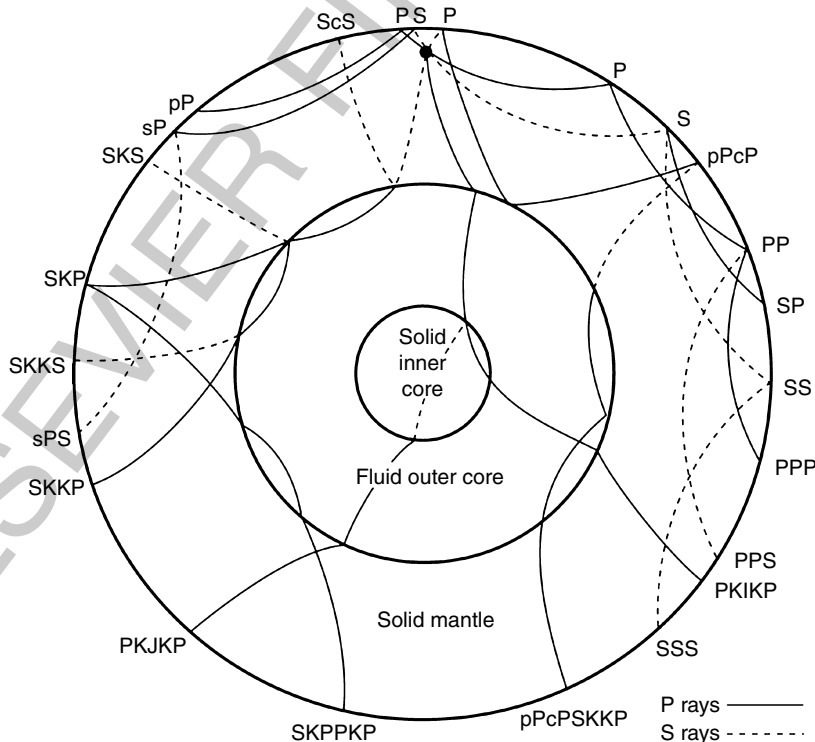


f0015 **Figure 3** Comparison of the seismic velocity models of Gutenberg and Jeffreys, both built in the 1930s. The principal difference between the models is the presence of the low-velocity zone in Gutenberg's model and the structure near the inner-outer core boundary; the low-velocity zone in the Jeffreys's model is erroneous and the velocity increase in the inner core is larger than in Gutenberg's model. With the exception of the transition zone (400–650 km depth) the modern models are not very different. From Anderson (1963).  
 AU24

propagate (K and I for the P waves in the outer and inner core, respectively; PKIKP designates a phase that travels as P in the mantle, P in the outer core, and P in the inner core), the boundary at which they were reflected (c for core–mantle boundary, i for the inner–outer core boundary). A shear wave reflected once from the free surface at the mid-point of its path is designated by SS; higher multiple reflections, like SSS or SSSSS, can be observed by sampling a large volume of the Earth along their paths. For earthquakes with a finite focal depth, the P and S waves traveling upward from the source have designation of p or s; following reflection at the surface they represent the so-called 'depth phases' (e.g., pP, sP); the traveltime difference between the arrival of pP and P strongly depends on focal depth.

Figure 4 shows examples of various seismic phases, and Figure 5 is the graphic representation of the traveltimes as a function of distance computed by Jeffreys and Bullen (1940) for the model of Jeffreys (1926). It is remarkable that this set of tables, including predictions for different focal depths, was calculated using a mechanical calculator! The data used by Jeffreys were extracted from the ISS, the precursor of the International Seismological Centre

p0080 With internal reflections and conversions of waves at the boundaries, seismologists developed a system of phase identification that reflects a combination of the types of waves (P or S), the region in which they



f0020 **Figure 4** Examples of seismic rays and their nomenclature. The most commonly identified phases used in earthquake location are the first arriving phases: P and PKIKP. From Stein and Wysession (2003).  
 AU25



## 6 Overview

and rare, and it was not until the 1960s that they became generally available at universities (Haskell worked at the Air Force Cambridge Laboratories).

p0105 Surface-wave dispersion began to be studied intensively in the 1950s principally at the Lamont Geological Observatory of Columbia University, primarily by Ewing and Press, who observed mantle waves in the 1952 Kamchatka earthquake, identifying arrivals from R6 to R15 and measuring their group velocities up to a period of 500 seconds (Ewing and Press, 1954). Regional measurements of surface-wave dispersion were initiated by Press (1956). A monograph by Ewing *et al.* (1957) summarizes the state of the knowledge on seismic-wave propagation in layered media at that time. Ewing and Press also developed a true long-period seismograph, which was capable of recording mantle waves even for moderately sized earthquakes. This instrument was deployed at 10 globally distributed International Geophysical Year network stations operated by Lamont.

p0110 It is not often that a mistake leads to favorable results, but this was the case with the free oscillations of the Earth. Benioff (1958) reported an oscillation with a period of 57 min seen in the record of the 1952 Kamchatka earthquake. Even though this observation was eventually attributed to an artifact in the functioning of the instrument, it stimulated the theoretical and computational research needed to calculate eigenfrequencies for a realistic Earth model. Some of the calculations preceded Benioff's report (Jobert, 1956, 1957), but the efforts of Pekeris and Jarosch (1958) and Takeyuchi (1959) were clearly motivated to explain the observed period. These calculations, using the variational approach and the Jeffreys–Bullen Earth model, predicted the period of  ${}_0S_2$  to be 52 min and that of  ${}_0T_2$ , 43.5 min; neither was close enough to Benioff's 'observation'. The modern approach was developed by Alterman *et al.* (1959), who recast the system of three second-order partial differential equations into a system of six first-order differential equations, thus removing the need for differentiation of the elastic constants and allowed the use of standard numerical methods to obtain the solution. Tests using Gutenberg's and Jeffreys–Bullen models showed that they predict very similar free oscillation periods for the gravest modes, but differ at shorter periods by 1–2%.

p0115 When the greatest instrumentally recorded earthquake of 20 May 1960 occurred in Chile, seismologists had all the tools (theory, computers, and instrumentation) needed to measure and interpret its recordings.

Three back-to-back papers in a 1961 issue of the *Journal of Geophysical Research* reported the first correct measurements of free oscillation periods: Benioff *et al.*, Ness *et al.*, and Alsop *et al.* The observations were made on strainmeters in Isabella, Ñaña, and Ogdensburg, seismographs at Pasadena, and a gravimeter at University of California, Los Angeles (UCLA). All three studies agreed in mode identification and found that their periods were very close to those predicted by the existing Earth models (Pekeris *et al.*, 1961a). More detailed studies of the spectra revealed that they are split, the effect of the Earth's rotation was shown to explain this effect (Backus and Gilbert, 1961; Pekeris *et al.*, 1961b). Thus normal-mode seismology was born. Progress in the theory, particularly considering the effect of lateral heterogeneities and mode coupling would extend over decades to come. First attempts at inversion of normal-mode data were not particularly successful; the density model of Landisman *et al.* (1965) was flat throughout the lower mantle, implying either a strong radial heterogeneity or an immensely superadiabatic gradient.

Backus and Gilbert (1967, 1968, 1970) provided the formal background for consideration of geophysical inverse problems, and even though their own experiments with inversion of normal-mode periods for the velocities and density, using a subset of normal-mode data, were discouraging (two very different models were found fitting the data nearly exactly; Backus and Gilbert, 1968), the idea of resolving kernels and tradeoffs became part of the geophysical terminology.

Seismic methods were considered essential in discriminating between earthquakes and nuclear explosions (Berkner *et al.*, 1959), and an intensive observational program, called VELA Uniform, was initiated. One of its components of great significance to studies of the Earth's interior was the World-Wide Standard Seismograph Network (WWSSN), consisting of a set of three-component short-period and three-component long-period seismographs, with identical responses, except for magnification, which depended on local noise levels. At its peak, the WWSSN consisted of 125 stations (Figure 6), with distribution limited by geography and politics: there were no stations in the Soviet Union, China, and poorly developed areas in Africa and South America. The novel aspect of WWSSN was its standardized response and centralized system of distribution of copies of seismograms. Individual stations were sending the original seismograms to a central location, where they were microfilmed, using a very

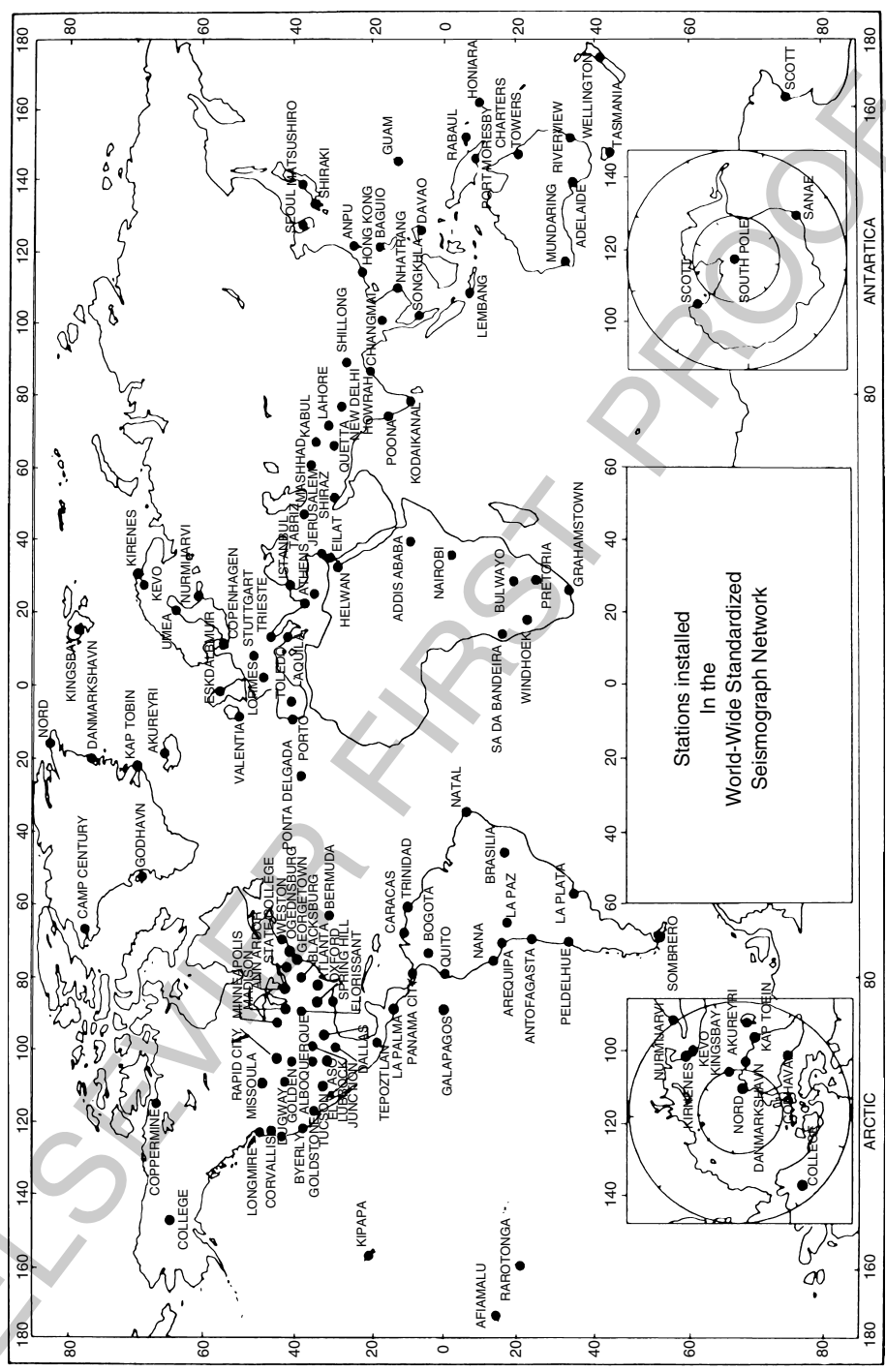


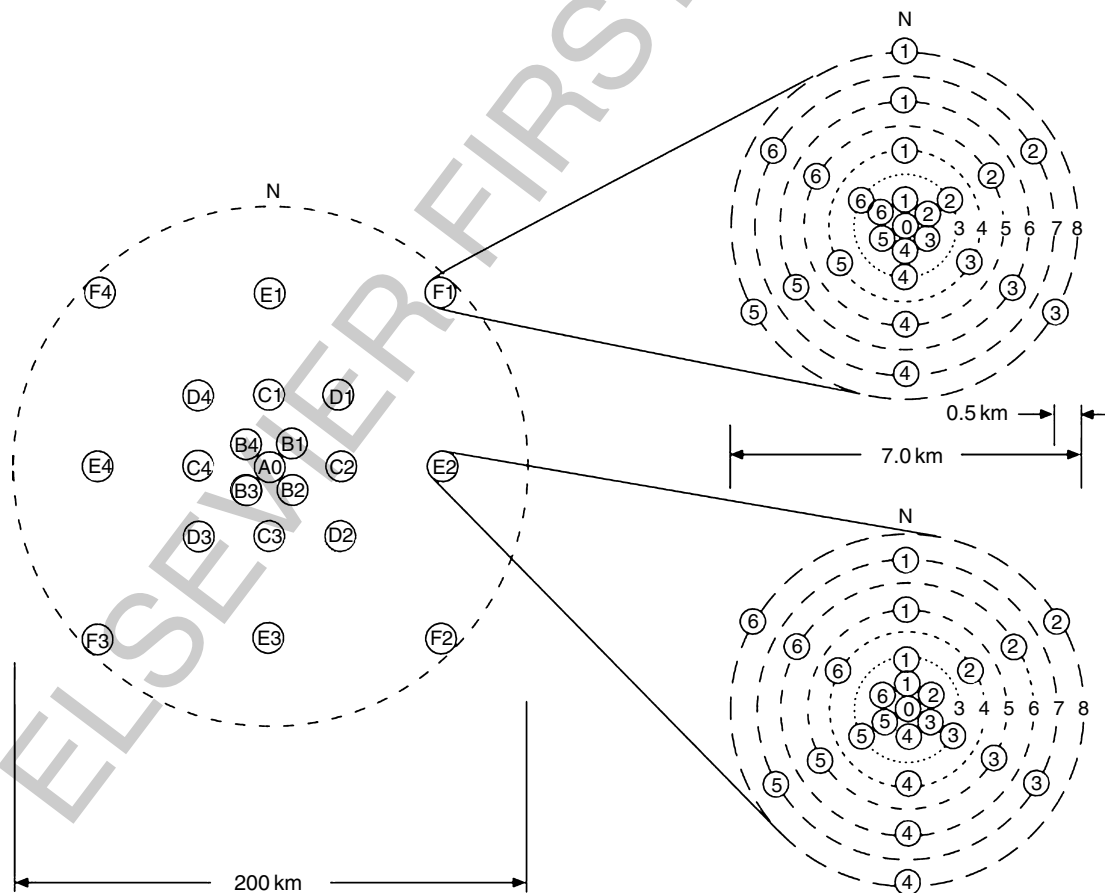
Figure 6 Map of the stations of World-Wide Standard Seismograph Network (WWSSN) established in the early 1960s, following recommendations of Berkner et al. (1959). Courtesy of US Geological Survey.

## 8 Overview

high-resolution camera, and then returned to the stations. A seismologist could request copies of seismograms for a particular date and receive them either as microfilm chips or photographic enlargements to the original size. Several larger institutions had a blanket order on all the records. This data accessibility represented major progress with respect to the earlier procedures, where one had to request copies of seismograms from individual stations, which greatly limited and delayed the research. WWSSN functioned for 20–25 years, slowly declining in the quality and number of stations; it ceased functioning in the late 1980s when data from new digital stations became available.

p0130 Another development of the 1960s was the introduction to seismology of digital recording, greatly facilitating research and the development of massive, computerized data-processing methods. One such facility, the Large Aperture Seismic Array (LASA), was built in the mid-1960s in Montana, shown in Figure 7. It contained six ‘rings’, for a total of 21

subarrays, each with 25 short-period seismometers emplaced in boreholes, to improve the signal-to-noise ratio. The data were telemetered in real time to a central location in Billings, Montana, where they were processed for detection of a signal. Major scientific discoveries were made with this tool, particularly when weak signals were involved; for example, observations of reflections from the inner core. In practical terms, the array did not meet the expectations; the site response across this 200 km aperture array varied so much that the signals had limited coherency and signal enhancement by stacking was not as effective as planned. A somewhat smaller array was installed a few years later in Norway (NORSAR); elements of this array are still active. Modern arrays used for seismic discrimination purposes have an aperture of only several kilometers, because on that scale, the coherency at 1 Hz frequency can be achieved. One of the important results obtained from the analysis of array data was the detection of upper-mantle



f003.5 **Figure 7** Configuration of the Long-Aperture Seismic Array (LASA) and an expanded view of two of its subarrays. From Stein and Wysession (2003).

**AU7** discontinuities (Johnson, 1966), confirming the result predicted by experimental petrology that there should be two discontinuities at pressures and temperatures corresponding to depths of about 400 and 650 km, respectively (Birch, 1952).

**AU8** **p0135** Surface-wave studies blossomed in the 1960s. At first, measurements of dispersion involved rather simple ‘analog’ methods, such as the peak-and-trough approach to measuring phase and group velocities. Some very important results were obtained in this way, such as the Canadian Shield study of Brune and

**AU9** Dorman (1963). Digital analysis, however, was soon to take over. Manual digitization of analog recordings, WWSSN data in particular, became easier, and with increasing availability of computers and decreasing cost of computations various techniques were developed, for the most part involving applications of the Fourier-transform technique. With the development of the fast Fourier transform (FFT) algorithm (Cooley and Tukey, 1965), the cost of time-series analysis declined dramatically; a review by Dziewonski and Hales (1972) summarizes the state of the art at the beginning of the 1970s. Some of these methods, such as the multiple filtration technique to measure group velocity dispersion, residual dispersion measurements, and time-variable filtration, are still in use today. The 1960s have also seen the first studies of intrinsic attenuation (Anderson and Archambeau, 1964), who developed partial derivatives for  $Q$  from mantle-wave attenuation. Also, the first studies of lateral heterogeneity were conducted using the ‘pure path’ approach (Toksöz and Anderson, 1966). Seismic experiments with controlled sources were conducted in a multi-institutional mode. One of the largest experiments was Early Rise, with up to 5 ton explosions in Lake Superior, with hundreds of seismometers spreading radially in all directions. Signals were recorded as far as 2500 km, reaching teleseismic distances and providing a detailed profile of P velocity under a continental upper mantle (Green and Hales, 1968); a detailed review of crustal and upper-mantle studies with controlled sources is provided in 00011.

**p0140** With a large new data set, particularly measurements of previously unreported periods of long-period overtones provided by the analysis of free oscillations generated by the 1964 Alaskan earthquake and recorded at WWSSN stations (Dziewonski and Gilbert, 1972, 1973), studies of 1-D structure entered a new era. The resolution of this data set was sufficient to constrain the density profile in the mantle and the core; this turned out to be quite

consistent with the behavior, in the lower mantle and outer core, of a homogeneous material under adiabatic compression. Jordan and Anderson (1974) were the first to combine the normal-mode and traveltime data, including differential travel data.

Numerous additional overtone data were obtained by Mendiguren (1973) and Gilbert and Dziewonski (1975) by introducing phase equalization techniques, such as ‘stacking’ and ‘stripping’. These methods require the knowledge of the source mechanism to predict the proper phase for each seismogram to be considered; this in itself turned out to be a challenging inverse problem. Dziewonski and Gilbert (1974) derived the spectrum of all six components of the moment-rate tensor as a function of time for two deep earthquakes (Brazil, 1963; Colombia, 1970). For both events, they detected a precursive isotropic component. Eventually, this turned out to be an artifact of coupling between toroidal and spheroidal (Russakoff *et al.*, 1998) modes, but the requisite theory to consider this effect was not available until 1984. Gilbert and Dziewonski (1975) presented two models based on measurements of eigenfrequencies of 1064 modes and mass and moment of inertia for a total of 1066 data. They derived two models 1066A and 1066B, with the first being smooth through the transition zone and the latter including the 400 and 660 km discontinuities.

At the 1971 General Assembly of the International Union of Geodesy and Geophysics (IUGG) in Moscow, the need for a reference Earth model was stated, and a Standard Earth Model Committee formed under the chairmanship of Keith Bullen. The Committee appointed several subcommittees, including one for the radius of the core–mantle boundary: there were discrepancies on the order of 10 km at the time. The value recommended by the subcommittee was 3484 km (Dziewonski and Haddon, 1974), which withstood the trial of time, within 1 km. Hales *et al.* (1974) proposed that the seismic velocities and density in the Standard Earth Model should be described by a low-order polynomial, with discontinuities at the appropriate depths. Dziewonski *et al.* (1975) constructed such a model, named Parametric Earth Model (PEM), which satisfied the normal-mode, traveltime, and surface-wave data. The novelty of this model was that, in single inversion, different structures were obtained for the continental and oceanic crust and upper mantle. The normal-mode periods predicted by these two models (PEM-O and PEM-C) averaged in 2/3 and 1/3

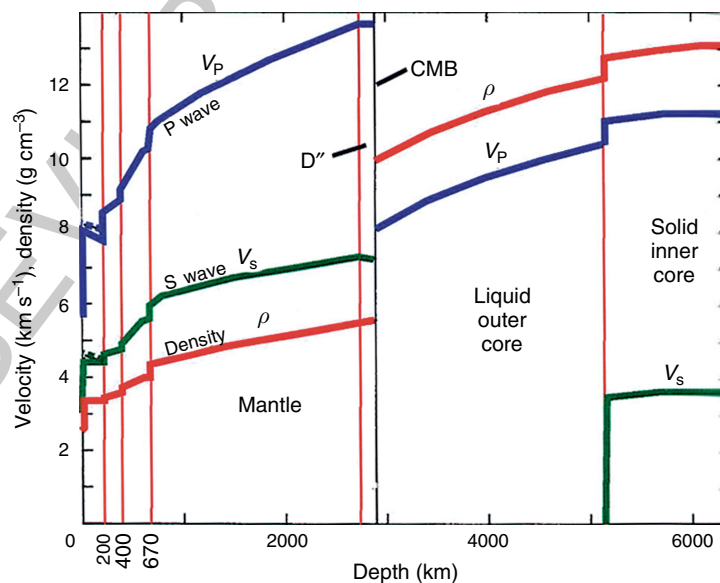
proportion were constrained to match the observed periods and teleseismic traveltimes, but separate data sets for continental and oceanic surface-wave dispersion. The differences between these two models ceased at the 400 km discontinuity, at which depth they became identical with the average Earth model, PEM-A.

p0155 The drawback of the PEM and all the previous models was that they did not consider the physical dispersion due to anelastic attenuation. For a signal propagating in an attenuating medium to be causal, the wave with higher frequencies must propagate with higher velocities. Thus waves with a frequency of 1 Hz will propagate more rapidly than waves at a frequency of 1 mHz. In order to reconcile the seismic data that span 3.5 orders of magnitude, it is necessary to consider the frequency dependence of elastic parameters. This was pointed out by Liu *et al.* (1976). The Preliminary Reference Earth Model (PREM) constructed by Dziewonski and Anderson (1981), following the idea of parametric representation, considered the frequency dependence using an assumption that  $Q$  is constant in the band from 0.3 mHz to 1 Hz.

p0160 This necessitated obtaining the radial profiles of  $Q_p$  and  $Q_s$ ; fortunately, there were new measurements available of normal-mode and surface-wave  $Q$  (Sailor and Dziewonski, 1978) such that a formal inversion

for  $Q$  could be conducted simultaneously with the inversion for the velocities and density. It was recognized earlier that to explain the observed attenuation of radial modes, which contain a very high percentage of compressional energy (97.5% for  ${}_0S_0$ ), it was necessary to introduce a finite bulk attenuation; Hart and Anderson (1978) preferred to place it in the inner core, AU10 Sailor and Dziewonski (1978) thought that  $Q_s$  is finite in the upper mantle; unfortunately, the radial modes do not have the requisite depth resolution. Figure 8 shows the seismic velocities and density as a function of radius; the attenuation in PREM is discussed in 00024. Another novel aspect of PREM was its radial anisotropy between the Moho and 220 km depth. This feature, at first suspected to be an artifact of the non-linearity of the inverse problem, has been confirmed by global tomographic studies (e.g., Ekström and Dziewonski, 1998). AU11

The 1970s have also seen the beginning of seismic tomography; two studies published simultaneously (Aki *et al.*, 1977; Dziewonski *et al.*, 1977) addressed the problem on different scales: regional and global. Aki *et al.* solved for 3-D velocity structure under the NORSAR array, while Dziewonski *et al.* obtained a very low resolution model of 3-D velocity perturbations in the entire mantle and showed significant correlation between velocity anomalies in the lowermost mantle and the gravest harmonics of the gravity p0165



f0040 **Figure 8** The Preliminary Reference Earth Model (PREM) of Dziewonski and Anderson (1981). In addition to the distribution of seismic velocities and density, PREM contains also the distribution of attenuation of the shear and compressional energy. From the web site of Ed Garnero.

field. The study of D<sup>b0145</sup>ziewonski *et al.* (1977) was motivated by a paper by Julian and Sengupta (1973) who noticed that traveltimes for rays bottoming in the same region of the mantle tend to show similar residuals; they interpreted this result qualitatively as the evidence of lateral velocity variations; no modeling was presented in that paper. The first continental-scale 3-D model of the upper mantle under North America was published by Romanowicz (1979).

p0170 Two digital seismographic networks were established in the mid-1970s. One was the International Deployment of Accelerometers (IDA; Agnew *et al.*, 1976, 1986), consisting of some 18 globally distributed Lacoste–Romberg gravimeters with a feedback system that allowed digitization of the signal. It was designed to record very long-period waves, including the gravest modes of free oscillations of the Earth: one sample was taken every 20 s (later changed to 10 s). Only the vertical component of acceleration was recorded and the word length was 12 bits; the dynamic range was, therefore, rather limited, but still considerably greater than that of analog recordings. The sensitivity was set such that the scale was saturated for the first surface-wave arrivals for events with magnitude 7.0, or so, depending on the station's distance from the source and radiation pattern. The IDA network was operated by the Scripps Institution of Oceanography and the centrally collected data were freely distributed to the academic community; this later became the future standard in global seismology. An early illustration of the power of such a global array was the analysis of splitting of the gravest modes of free oscillations generated by the 1977 Sumbawa earthquake (Buland *et al.*, 1979; *M<sub>w</sub>* only 8.4).

AU12

p0175 The other network consisted originally of nine installations called Seismic Research Observatories (SRO) and five Abbreviated Seismic Research Observatories (ASRO). The SROs were borehole instruments, with significantly suppressed wind-generated noise levels particularly on horizontal components. The ASROs were placed in underground tunnels or mine shafts and the seismographs were protected from the effects of changing pressure and temperature. The instrumentation is described by Peterson *et al.* (1976). This network was designed for monitoring the Nuclear Test Ban Treaty and high sensitivity was the main objective. In order to increase the dynamic range, the signal was sharply band-pass-filtered, so that at very long periods (>200 s) the response to acceleration was falling as  $\omega^{-3}$ , while it was flat for the IDA instruments. Even so, the SRO and ASRO stations were able to produce

useful mantle-wave records for events with magnitude greater than about 6.5. Later, the network was augmented by 10 WWSSN stations, with the analog output amplified and digitized using 16-bit digitizers. The entire system was called Global Digital Seismographic Network (GDSN). There was no general data distribution system, but data for selected dates were available upon request from the Albuquerque Seismological Laboratory.

Until then, a seismic station typically comprised a p0180 set of seismometers with either 'long-period' or 'short-period' responses, or sometimes, as was the case for the WWSSN, one of each. This setup was designed at the time of analog recording to avoid the microseismic noise peak around 6–7 s period, which would have made it impossible to digitize all but the largest earthquake signals. With digital recording, and the possibility of filtering out the microseismic noise by postprocessing, this traditional instrument design became unnecessary.

A very important development in seismic instrumentation thus took place in Germany in the mid-1970s. An array of a new kind of instruments with digital recording was deployed near Gräfenberg (Harjes and Seidl, 1978). It used a novel feedback seismograph (Wielandt and Streckeisen, 1982). The system was rapidly recognized for its linearity and large dynamic range within a wide band of frequencies – hence the name 'broadband'. The Gräfenberg array's central station had been co-located with the SRO borehole station GRFO, and the comparisons were very favorable for the broadband instruments, which were capable of reproducing different narrow-band responses using a single data stream. This type of instrumentation became the pattern for future developments.

In addition to the developments in instrumentation, p0190 the late 1970s saw important theoretical developments, related to the asymptotic properties and coupling of the normal modes. Examples of such developments are papers by Woodhouse and Dahlen (1978), Jordan (1978), and Woodhouse and Gernius (1982).

AU13

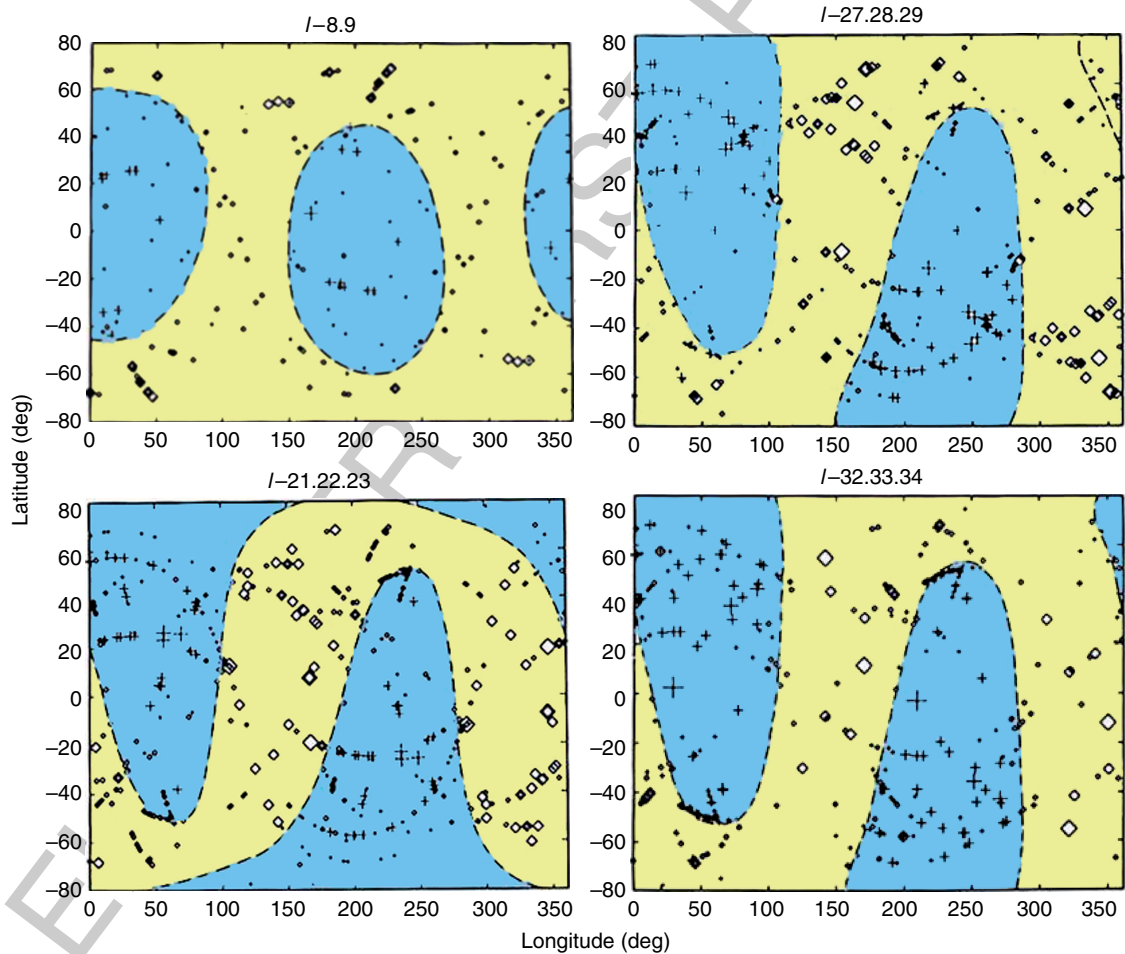
### 1.01.3 From 1980 to Present: The Era of Tomography and Broadband Digital Seismic Networks s0015

The data from both global networks of the 1970s led p0195 to results that demonstrated the need for development of a global network that would better satisfy the needs of basic research in seismology; three studies

## 12 Overview

are noteworthy. A robust method, which uses entire segments of (digital) seismograms, was developed to obtain reliable mechanisms of earthquakes with magnitude 5.0 and above (Dziewonski *et al.*, 1981; Ekström *et al.*, 2005). In addition, the method refines the location of the source, which for an event of finite size need not be identical with the hypocenter determined from the first arrivals of the P waves. This topic is discussed at length in 00077. The reason that the subject is brought up here is that in most aspects of using waveform analysis for the purpose of drawing inferences about the Earth's structure, it is necessary to know the source mechanism. The so called 'centroid-moment tensor' method has now been applied to over 25 000 earthquakes from 1976 till present, and this catalog is available online.

Masters *et al.* (1982) measured center frequencies of spectral peaks of the fundamental spheroidal mode from hundreds of IDA records and discovered that there are spatially distinct patterns in the frequency shifts when plotted at locations of the poles of the great circles corresponding to the paths between the source and receiver. By fitting spherical harmonics (even degrees only, because of the symmetry) these authors realized that the pattern is dominated by spherical harmonics of degree 2, an observation also made from great-circling surface waves by Souriau and Souriau (1983). Figure 9 shows the pattern of the shifts of spectral peaks and zero line of the best-fitting spherical harmonics of degree 2 for four groups of  ${}_0S_\ell$  modes with different ranges of degree  $\ell$ . Note that the modes with the lowest  $\ell$  show a different pattern



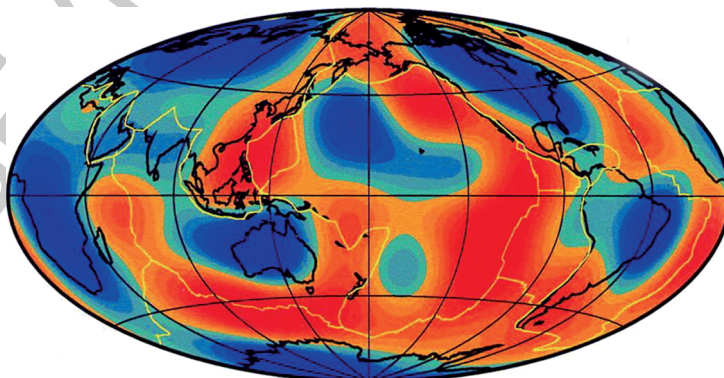
f004.5 **Figure 9** Maps of the observed frequency shifts of the fundamental spheroidal modes for four ranges of the order numbers as reported by Masters *et al.* (1982). The frequency shifts are plotted at the poles of the individual great-circle paths. It indicates the presence of very large wavelength-velocity anomalies in the Earth's interior; the preferred location of the source of the anomaly shown in the figure is the transition zone. Modified from Masters G, Jordan TH, Silver PG, and Gilbert F (1982) Aspherical Earth structure from fundamental spheroidal mode data. *Nature* 298: 609–613.

than the remaining three groups. Our current understanding of this fact is that the low- $\ell$  modes sample deeper structure (lower mantle) than the higher- $\ell$  groups which predominantly sample the upper mantle. The authors performed a parameter search, in which they changed the radii of a shell in which the anomaly is located. The best variance reduction was for the anomaly placed in the transition zone. The lasting importance of this paper is that it demonstrated that heterogeneity of very large wavelength and sizeable amplitude ( $\pm 1.5\%$ ) exists in the Earth's interior.

**p0205** Following the development of a waveform-fitting technique that allowed a simultaneous measurement of the phase velocity and attenuation along a great-circle path (Dziewonski and Steim, 1982), **AU14** Woodhouse and Dziewonski (1984) developed an approach to interpretation of waveforms that could extract both the even- and odd-harmonic coefficients of lateral heterogeneity as a function of depth. Their method involves the 'path average approximation', sometimes called PAVA. The seismograms are represented as a sum of all normal modes (spheroidal and toroidal) up to a certain frequency  $\omega_{\max}$ . For a given great circle, each mode is assumed to be affected by the average deviation from reference structure along the great-circle path (which is sensitive only to even-order harmonics), and along the minor-circle path (sensitive to both even- and odd-harmonics). The effect of the great-circle path can be modeled by a shift in eigenfrequency of the mode; the effect of the minor-arc structure is modeled by a fictitious shift of the epicentral distance for that mode; this shift

depends on both even and odd part of the structure. Woodhouse and Dziewonski (1984) processed about 2000 mantle-wave seismograms from the GDSN and IDA networks and obtained a model of the upper mantle (Moho – 670 km), M84C, using as basis functions spherical harmonics up to degree 8 for horizontal variations, and Legendre polynomials as a function of radius up to degree 3. **Figure 10** shows a map of shear-velocity anomalies at a depth of 100 km; there was no *a priori* information used on the location of the plate boundaries. Corrections were made for crustal thickness, recognizing only the continental and oceanic structure. An experimental model, M84A, obtained without applying crustal corrections, showed that not taking crustal thickness into account may result in mapping artificial anomalies at depths as large as 300 km. Model M84C had a strong degree-2 anomaly in the transition zone, confirming the results of Masters *et al.* (1982).

Another result also affected future developments, **p0210** even though this study was not based on waveform analysis, but on the ISC bulletin data. With greater computational resources, it was possible to cast the inverse problem for lateral heterogeneities in the lower mantle on a larger scale using a substantially greater body of data than in Dziewonski *et al.* (1977). Unlike in this earlier study, in which blocks were used, Dziewonski (1984) used global functions: spherical harmonics representing horizontal variations and Legendre polynomials for radial variations. The degree of expansion was modest: only degree 6 in harmonics and degree 4 in radius, with the inversion limited to lower-mantle structure. In many ways, this



**f00.50** **Figure 10** Shear-velocity anomalies at a depth of 100 km in the model M84C of Woodhouse and Dziewonski (1984). The scale range is  $\pm 5\%$  and the resolving half-wavelength is 2500 km. Except for the correction for crustal thickness, there was no additional *a priori* included in the inversion, so the result demonstrates that the waveform inversion approach is able to distinguish the slow velocities under the mid-ocean ridges and ancient cratons, for example.

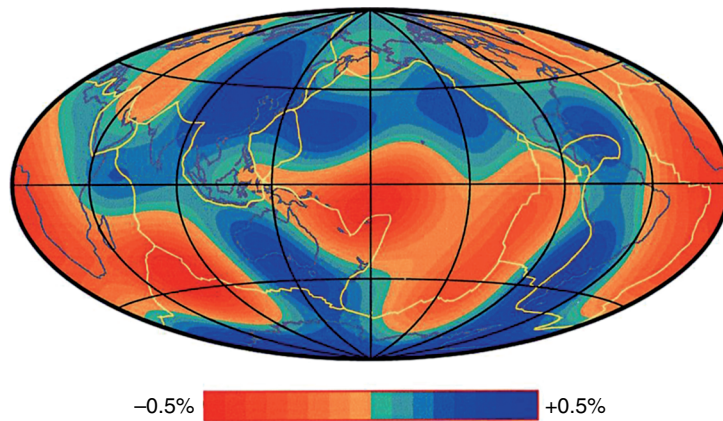


**Figure 11** Map of P-velocity anomalies at a depth of 2500 km in model of Dziewonski (1984) derived from inversion of traveltime anomalies from ISC Bulletins. The resolving half-wavelength of the model is about 3500 km (at the surface). The model, dominated by the harmonics 2 and 3, clearly shows two large superplumes (African and Pacific) and the ring of fast velocities circumscribing the Pacific rim. The scale is  $\pm 0.5\%$ .

new study confirmed the earlier one – including the correlation of lower-mantle structure with the gravity field – but it allowed resolution of a truly remarkable concentration of the power of heterogeneity in low-order harmonics. **Figure 11** shows a map of P-velocity anomalies at a depth of 2500 km. The structure, dominated by degree 2 (and, to a lesser extent, degree 3) shows two large slow regions, which came to be known as the African and Pacific ‘superplumes’, and a ring of fast velocities around the Pacific.

Thus seismology demonstrated that it can resolve 3-D structure within the Earth interior, giving the promise of an unprecedented ability to look at a present-day snapshot of mantle dynamics. Yet, the observing networks were in decline, with the support for the GDSN likely to be discontinued altogether, and the original IDA network (limited to recording of vertical-component mantle waves and free oscillations) not meeting the needs of the broader community. In 1983, a plan was put forward to create a Global Seismographic Network (GSN) of some 100 broadband, three-component seismographic stations sending the data in nearly real time to a central collection facility. The expectation was that this network would be supported by the National Science Foundation (NSF), in analogy to NSF supporting astronomy facilities. At the same time, seismologists using portable instrumentation came to the realization that they needed a centralized and standardized instrument pool. This led to formation of a project called Portable Array for Seismological Studies of

Continental Lithosphere – PASSCAL. The GSN and PASSCAL groups merged and formed a consortium known as Incorporated Research Institutions for Seismology (IRIS), which incorporated in 1984.

At the same time, Steim (1986) was developing at Harvard his very-broadband (VBB) instrument, based on the STS-1 broadband seismograph (Wielandt and Steim, 1986), and a very high-resolution (24-bit) digitizer. The response of a VBB instrument is designed to have a flat response to ground velocity between 5 Hz and 3 mHz, that is, over more than three orders of magnitude. Such an instrument had to have a very large dynamic range, of about 140 dB to span the range of ground velocities from the minimum Earth noise to a magnitude 9.4 earthquake at  $30^\circ$  epicentral distance. All these requirements were met, and Steim’s VBB system became the design goal for the GSN and other networks. **Figure 12** shows the operating range of the system and **Figure 13** illustrates the dynamic range of the GSN station in Albuquerque. The high-pass-filtered (75 s) record of the Sumatra-Andaman  $M_w=9.3$  earthquake shows surface waves with an amplitude of several millimeters and a record of a local microearthquake ( $M < 1$ ) extracted from the same record; the ratio of the amplitudes is about 10 000 000!

Meanwhile, as the US seismologists were organizing themselves, a French effort named Geoscope had already begun taking shape; the objective being the establishment of a global network of some 20–25 broadband digital seismographic stations utilizing

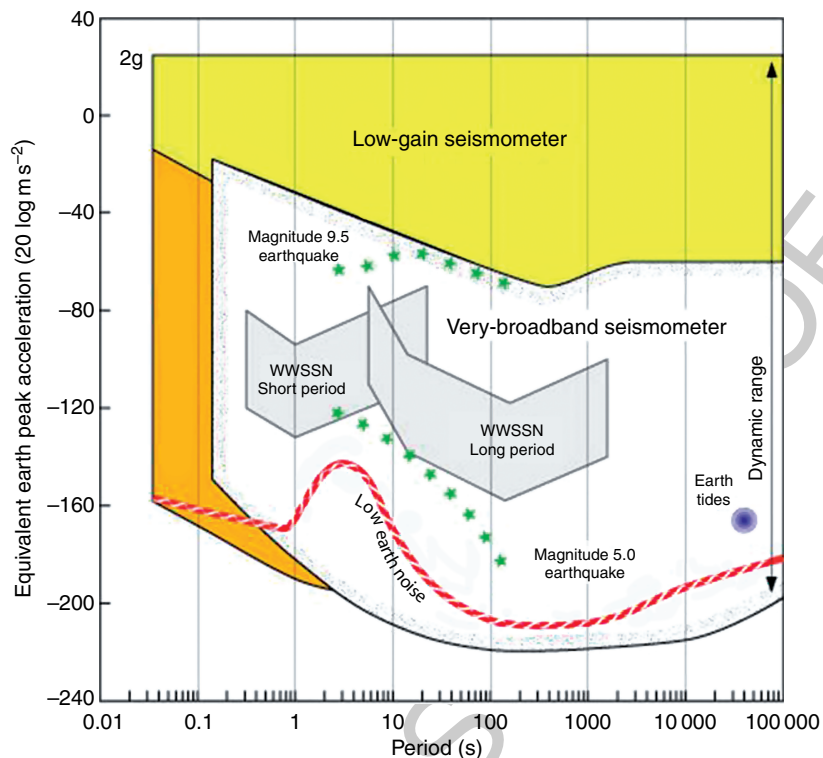
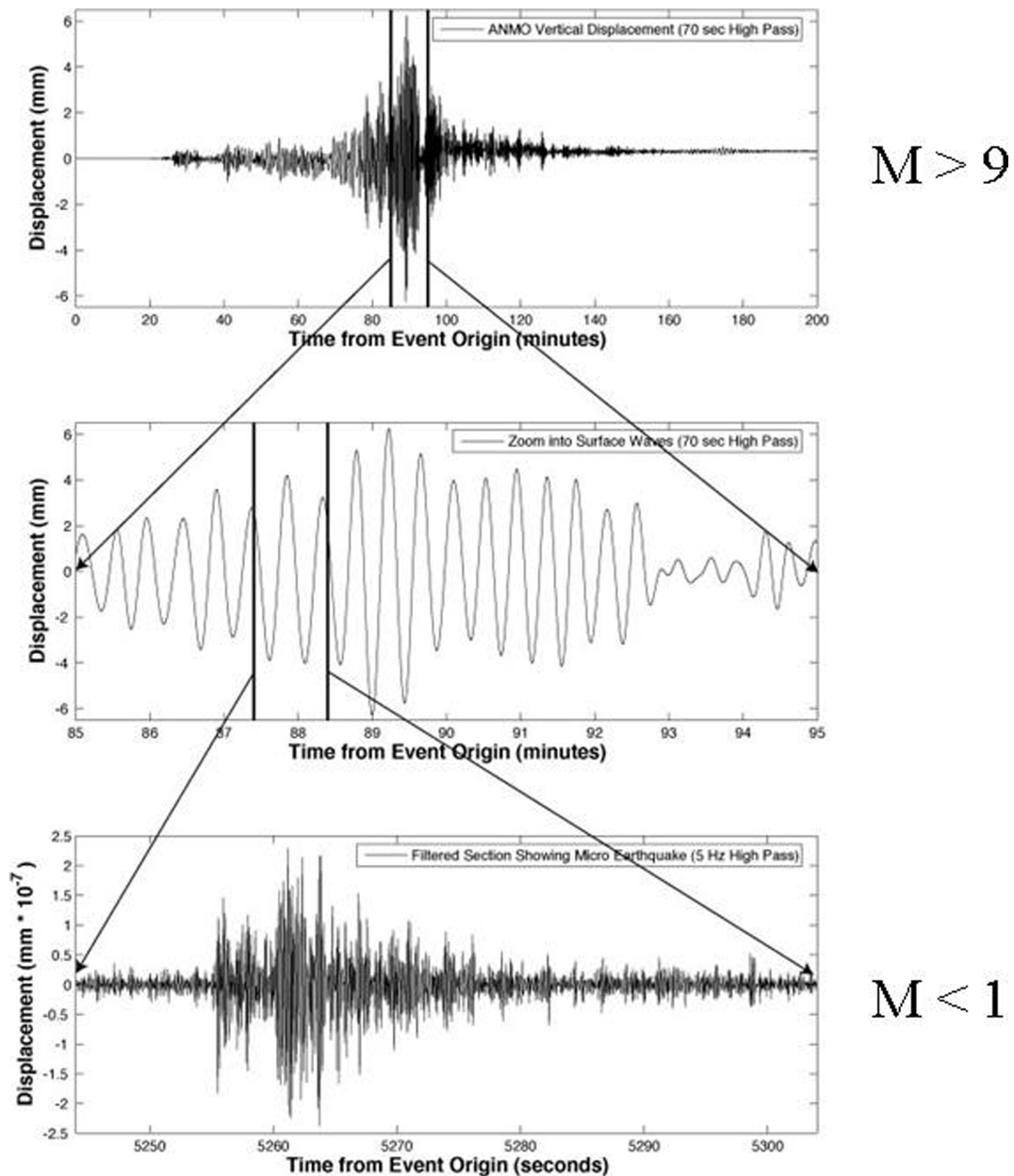


**Figure 12** The dynamic range of the VBB channels of a Global Seismographic Network station. The range of the WWSSN short- and long-period channels are shown for comparison. At some GSN stations the VBB channels are augmented by very short-period channels and accelerometers. The response was designed to resolve the ground noise from 5 Hz to tidal frequencies and to record on scale a magnitude-9 earthquake at a distance of  $30^\circ$ . Courtesy of Rhett Butler.

the STS-1 seismometer, and destined in priority for locations around the world that filled gaps in the distribution of seismic stations. The project had officially begun in 1982 and in 1984 there were already five operational stations (Romanowicz *et al.*, 1984), and 13 in 1986. While telemetry of the data was established later (in 1987), from early on, state of health of the remote stations was monitored using the satellite system Argos, which greatly facilitated their maintenance. As it was clear that it was inefficient to have two competing global networks, the need for a framework for international cooperation arose. Also, many countries were interested in deploying broadband instrumentation for their national or regional purposes, and were agreeable to share these data. A Federation of Digital Seismographic Networks (FDSN) was formed in 1986 (Romanowicz and Dziewonski, 1986), with the purpose of coordinating site selection, data exchange, and standardizing instrument responses. The FDSN has been very successful in achieving these goals, despite the fact that it is a purely voluntary, zero-

budget organization. **Figure 14** shows a map of the FDSN network as of January 2007 (after some 25 years of development); there are over 200 participating VBB stations, most of which now send data in nearly real time.

Similarly impressive progress was made in the area of field seismology, where progress in electronics led to overall improvement of the portability of the equipment and, in particular, reduction of power requirements, which makes operations much easier. In parallel with the development of the PASSCAL program of IRIS in the US (*see* 00015), other portable arrays were developed in other countries in the last 20 years, such as the Lithoscope program in France (Poupinet *et al.*, 1989) or the SKIPPY array in Australia (van der Hilst *et al.*, 1994). Most recently, an ambitious program, USArray, was launched in the US as part of the Earthscope project. USArray is aimed at a systematic, investigation of the structure under the contiguous United States with uniform resolution. It consists of three parts: a Permanent Array of



f0065 **Figure 13** Illustration of the dynamic range of a VBB station (ANMO). A recording of a local microearthquake with magnitude below 1 is extracted from the record dominated by the minor-arc surface waves generated by the Sumatra-Andaman magnitude-9.3 event. Courtesy of Rhett Butler.

AU26

100 stations (the ‘backbone’ or ‘reference array’), a Transportable Array (TA), and a Flexible Array (FA). The FA will provide some 300 broadband seismographs and over 1000 active-source instruments, for experiments proposed by individual research groups, aimed at elaborating detailed local structure. The TA is the largest component of the program and it consists of 400 broadband

seismograph systems, that will move gradually across the continental US over a 7-year period, to cover the entire area with, roughly, 2000 deployments for up to 2 years in a given location; the average instrument spacing is 70 km. The ‘reference array’ will provide the means to relate the waveforms recorded at different stages of TA deployment. Many other portable networks for regional studies of the crust and

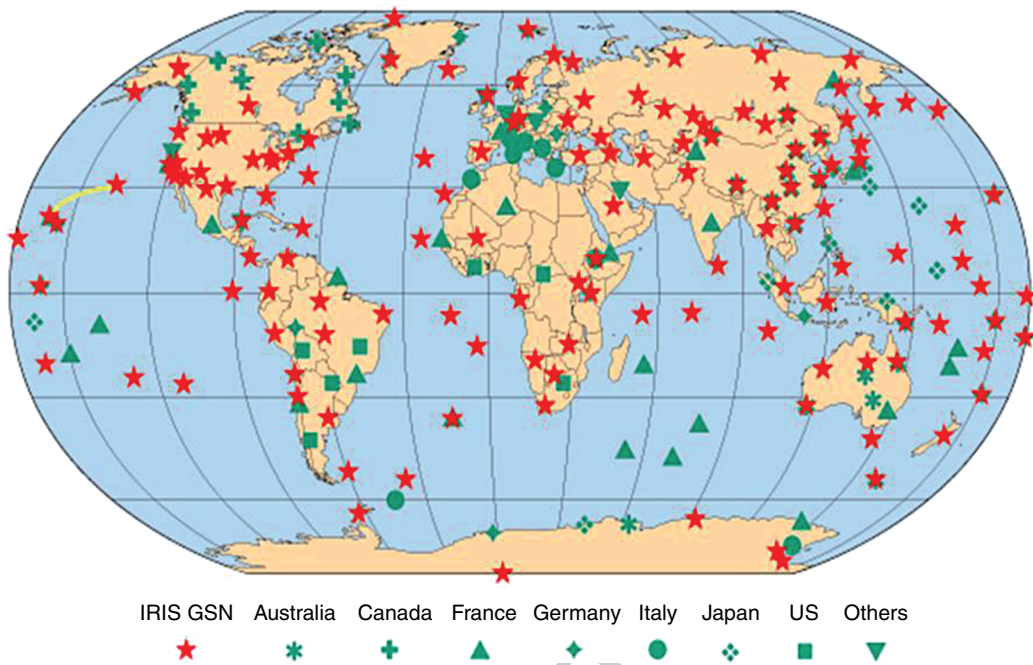


**Figure 14** Current (January 2007) map of the stations of the Federation of Digital Seismographic Networks. Stations of different member networks are identified by symbols shown at the bottom. Courtesy of Rhett Butler.

lithosphere using passive and active sources have been developed and deployed in the last 20 years (*see* 00011, 00015, 00016).

we have been obtaining models whose reliability is difficult to assess. **Figure 15** illustrates an example of how the results can be altered with the change of parametrization. A set of about 40 000 phase-delay data for Rayleigh wave with 75 s period (Ekström *et al.*, 1997) is inverted for ‘local’ phase velocities. The top panel of **Figure 15** shows the result in which the data were inverted for a set of basis functions represented by spherical harmonics up to degree 16; this requires solving for 289 unknown coefficients. Because the data set is so large and the global coverage is good, the solution was obtained by an exact matrix inversion. The results look reasonable, without any indication of instability. The lower panel of **Figure 15** shows the result obtained using a  $2^\circ \times 2^\circ$  block expansion, which requires solving for approximately 10 000 unknown values. Matrix conditioning was required in this case, and it was accomplished by applying combined norm and roughness damping. What is clear from the ‘high-resolution’ solution, is that the amplitudes are generally lower and there are ‘streaks’ indicating artifacts caused by uneven sampling of the area. What is difficult to find, however, are any features that appear to be significant that are not present in the solution with 30 times fewer parameters.

#### s0020 **1.01.4 Current Issues in Global Tomography**

p0235 In parallel with instrument development, scientific progress in seismic tomography has been rapid during the last 20 years, and most of the accomplishments are summarized in two reviews by Romanowicz (1991, 2003), as well as in 00009 and 00018. However, there are still issues that remain unresolved or controversial. Certainly, there are confusing observations related, for example, to anisotropic properties or differential rotation of the inner core, the core–mantle topography, anti-correlation of density and shear velocity near the bottom of the mantle, the strength and depth distribution of anisotropy in the Earth’s mantle, and the role of the post-perovskite phase change in mantle dynamics.

p0240 But the foremost issue in our view relates to the derivation and interpretation of 3-D Earth models. Ever since it was discovered that inversion of ill-conditioned matrices can be dealt with by requiring minimization of the norm or roughness of the model,

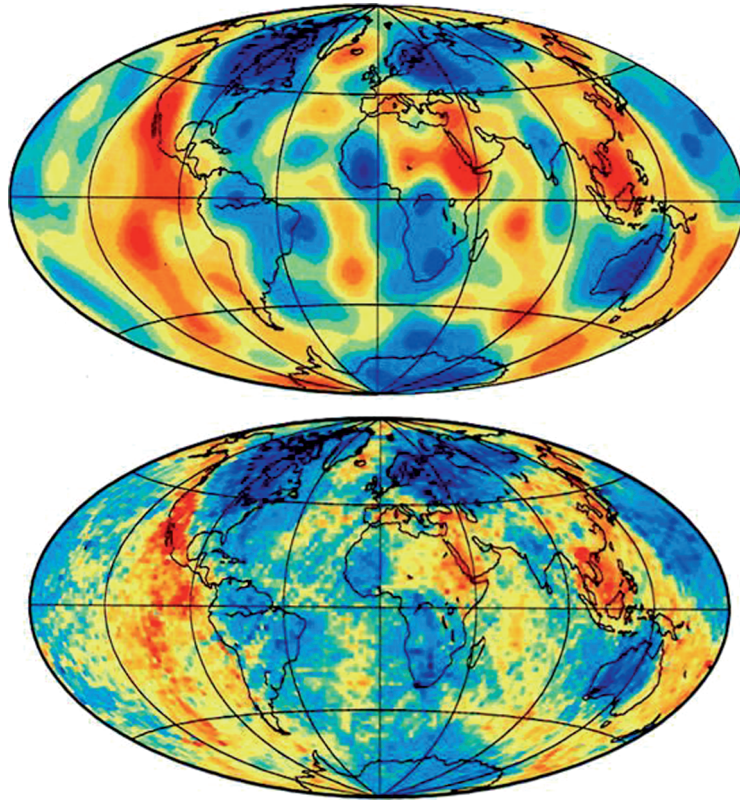


**Figure 15** Demonstration of the results of inversion of the same data set (40 000 phase delay data for 75-s Rayleigh waves measured by Ekström *et al.*, 1997) for different numbers of parameters. The top map shows inversion for spherical harmonic coefficients up to degree 16 (289 parameters). The bottom map shows the results of inversion for about 10 000 equal-area blocks; in this case matrix conditioning is necessary. The amplitude of the anomalies is lower, artifacts of an uneven path distribution are visible (e.g., across the central Atlantic) and it is difficult to find features that have not been resolved by the top map. The conclusion is that there is a price for unduly increasing the number of unknowns. Courtesy of L. Boschi.

Thus, sometimes, less is better. There is no absolute rule; the answer depends on the character of power spectra of a particular function. **Figure 16** shows results from Su and Dziewonski (1992) which indicate that spectra of several global functions, such as free-air gravity, continent–ocean function, or SS-S traveltime residuals, have a power spectrum that is relatively flat up to degrees from 6 to 8, after which it begins to decrease as  $\ell^{-2}$ . This seems typical of the spectra of 2-D functions that are characterized by a set of large ‘patches’, such as the large land masses in the continent–ocean function. If the spherical harmonic expansion is truncated at an order number beyond the corner wave number, the synthesis of such truncated series retains the main character of the original function (see figure 5 in Woodhouse and Dziewonski (1984), for an example of the continent–ocean function truncated at degree 8). Similarly, an inversion for a truncated series of spherical harmonic

coefficients does not introduce aliasing if truncation occurs in the steeply decreasing part of the power spectrum. There are some geophysically important functions whose spectra have distinctly different characters; for example, linear features (slabs) have power spectra that are flat with harmonic order, point-like features (plumes) have power spectra whose values increase with  $\ell$ . In these cases, truncation would result in significantly lower amplitudes in the low-pass-filtered image.

The issue of parametrization is an important one, particularly if the global behavior of the solution is to be preserved. **Figure 17** illustrates cross sections of four global P-velocity models – derived from the same data source (ISC Bulletins) – that span 3 orders of magnitude in the number of parameters. Clearly, there is not a simple relationship between the number of parameters and information contained in the model. It is so, partly, because the lower-mantle

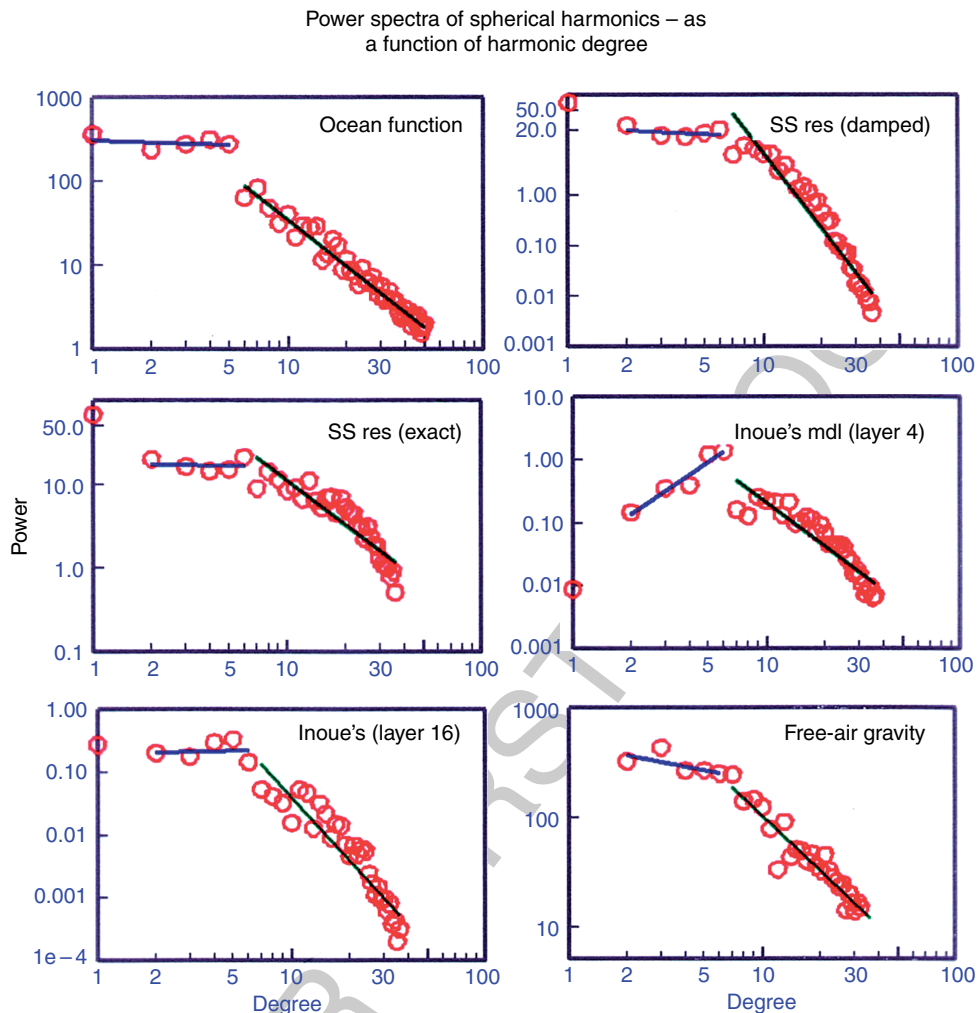


**Figure 16** Illustration of the power spectra for several global functions, including two layers from a P-velocity model of Inoue *et al.* (1990). Most of the functions shown have a flat power spectrum at low-order numbers and rapidly decreasing power above degrees 6–8. The practical result of such a property of the spectra is that truncation of the expansion at an order number corresponding to the steeply decaying power does not alias inversion results at low-order numbers (Su and Dziewonski, 1991, 1992). After Su W-J and Dziewonski AM (1992) On the scale of mantle heterogeneity. *Physics of the Earth and Planetary Interiors* 74: 29–54.

spectrum is dominated by the very low degrees that are fully recovered by the degree-6 model.

Another important issue in assessing global, as well as regional, tomographic models is the data set (or subsets) and the resolving properties that were used to derive them. The mantle models derived using only teleseismic traveltimes, for example, have very little radial resolution in the upper mantle, because the ray paths do not bottom there. The teleseismic traveltimes are sensitive to velocity perturbations in the upper mantle, but the variations with radius cannot be resolved above the lower

mantle. For example, all maps of upper-mantle velocity anomalies in **Figure 18** show that a model derived using only teleseismic traveltimes have slow velocities under the mid-ocean ridges at all upper-mantle depths, simply from the smearing with depth of the large slow anomalies occurring near the surface.

Models built using teleseismic traveltimes and fundamental-mode dispersion data do not have sufficient resolution in the transition zone to distinguish its unique properties. Only three research groups involved in whole-mantle modeling

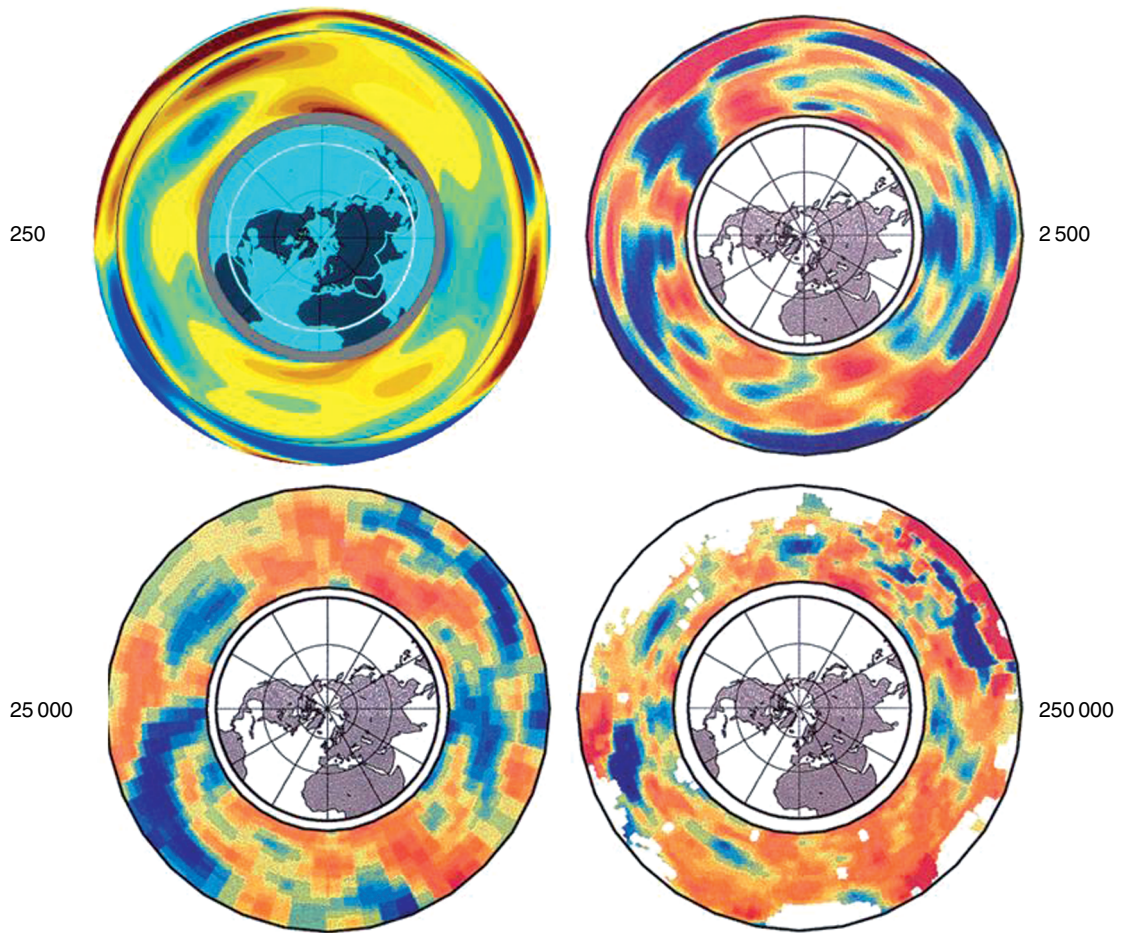
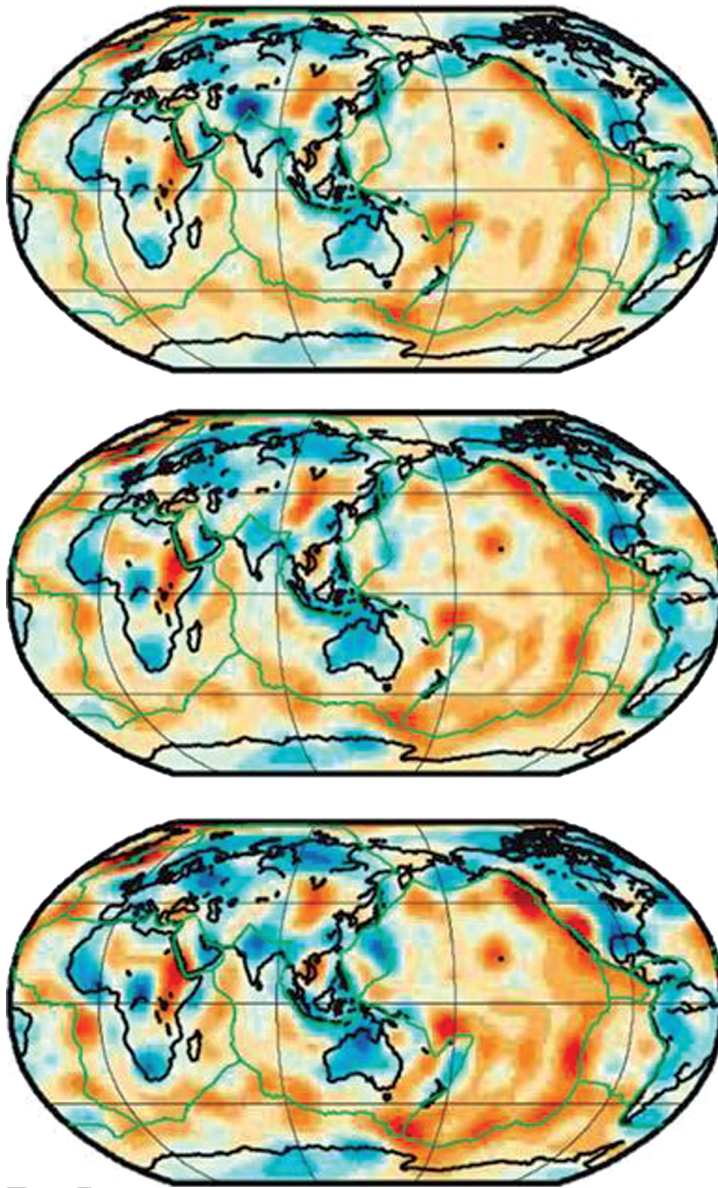


**Figure 17** Comparison of the equatorial cross-sections of four P-velocity models obtained by inversion of traveltimes residuals from ISC Bulletins using a number of unknown parameters that cover three orders of magnitude. The image of the African and Pacific superplumes is clearly seen in the model derived by using 250 parameters, while it could not be readily inferred from the model that used 250 000 parameters. The models obtained using 2500 and 25 000 parameters support the conclusion drawn in **Figure 16**. Modified from Boschi L and Dziewonski AM (1999) ‘High’ and ‘low’ resolution images of the Earth’s mantle – Implications of different approaches to tomographic modeling. *Journal of Geophysical Research* 104: 25567–25594.

(Caltech/Oxford, Berkeley, and Harvard) use data allowing sufficient resolution in this region; it is interesting that they derive this information differently, therefore adding to the credibility to the results. The use of waveforms in deriving 3-D models was pioneered by Woodhouse and Dziewonski (1984), but in the original paper only data with periods longer than 135 s were used. Long-period body waves were used in inversion by Woodhouse and Dziewonski (1986, 1989). Dziewonski and Woodward (1992) combined waveforms and teleseismic traveltimes measured by Woodward and Masters (1991). The immediate result was that the two models they derived showed a sudden change in the

pattern of heterogeneities across the 670 km boundary, and this was pointed out and discussed by Woodward *et al.* (1994). Later inversions by the Harvard group included also surface-wave dispersion data reported by Ekström *et al.* (1997). This increased resolution near the surface but did not alter the behavior across the upper–lower mantle boundary (Gu *et al.*, 2001, 2003; Kustowski *et al.*, 2006). All these models were obtained using the PAVA, which assumes constant average structure along the raypath. The Berkeley group pioneered use of a more advanced theory called nonlinear asymptotic coupling theory (NACT) first described by Li and Romanowicz (1995) and based on the across-branch



f0090 **Figure 18** A fragment of a figure from Ritsema *et al.* (2004) illustrating a typical result of an upper-mantle structure obtained using teleseismic traveltimes, whose rays do not bottom in the upper mantle. The three maps show smeared-out structure from near the top of the mantle (mid-ocean ridge anomalies). The conclusion drawn from the full figure (see 00009) is that, to obtain a whole-mantle model, one should use diverse types of data. Modified from Ritsema J, van Heijst HJ, and Woodhouse JH (2004) Global transition zone tomography. *Journal of Geophysical Research* 109: B02302 (doi:10.1029/2003JB002610).

coupling asymptotic development of Li<sup>b0325</sup> and Tanimoto (1993). This theory allows to construct kernels that give good representation of the sensitivity along and around the raypath as shown in **Figure 19**. In applying NACT to the development of several generations of global mantle models (Li<sup>b0335</sup> and Romanowicz, 1996; Mègnin and Romanowicz,

1999), most recently including attenuation (Gung and Romanowicz, 2004) and radial anisotropy (Panning and Romanowicz, 2006), the Berkeley group divided the seismograms into wave packets containing one or several body waves or surface-wave overtones, which allowed them to weigh different phases differently in order to obtain uniform

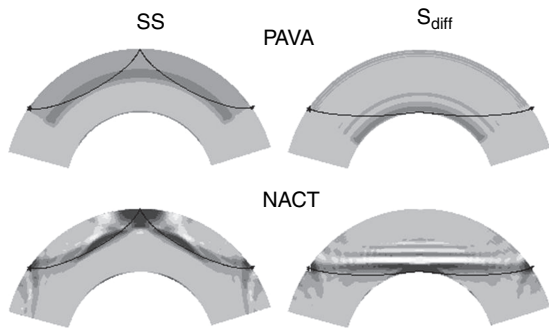


**Figure 19** Comparison of sensitivity kernels in the vertical plane containing the source and the receiver for SS waves (left) and  $S_{\text{diff}}$  waves (right), using the Path Average approximation (PAVA, top) and the non-linear asymptotic coupling theory (NACT, bottom). PAVA produces 1D kernels, which do not represent well the ray character of body waves. NACT, which includes across-branch mode coupling, produces 2D finite frequency kernels that more accurately represent the sensitivity along and around the ray path as well as its variations with position along the ray. The NACT kernels are time dependent and are here represented at a particular point in the waveform, with positive maxima in black and negative ones in white. Shadows beyond the source and receiver are due to the truncation in the coupling series. Adapted from Li and Romanowicz (1995).

sensitivity with depth. The Berkeley group does not use traveltimes explicitly, but information on structure is included in the phase of a waveform of, for example, an SS arrival. Thus, a large collection of waveforms containing images of phases such as S, SKS,  $S_{\text{diff}}$ , Love, and Rayleigh fundamental and overtone waves will represent similar information as the combination of teleseismic traveltimes and surface-wave phase velocities in Caltech/Oxford or Harvard models. In addition, unlike traveltime analysis, wave packets containing several phases with close arrival times but different sampling of mantle structure, can be included, improving resolution. An important element of the data set used by Ritsema *et al.* (1999) is a set of maps of Rayleigh wave overtone dispersion from the first through fifth overtones. These were obtained by ‘stripping’ the seismograms of subsequent overtones, thus providing the data on the average phase velocity of a particular overtone between the source and receiver (van Heijst and Woodhouse, 1997). Since body waves represent superposition of overtones, use of complete waveforms is, to a large extent, equivalent; however, the separation of data for individual overtones allows assignment of different weights to different

overtones, while direct waveform methods use them with the weight that is determined by their excitation; generally, the amplitude of overtones decreases with the overtone number. On the other hand, waveforms contain information about all the overtones. The importance of the overtones (body-wave waveforms) was shown implicitly by Gu *et al.* (2001) and explicitly by Ritsema *et al.* (2004). The importance of using adequate kernels for overtone and body waveforms was illustrated by Mégnin and Romanowicz (1999) in a comparison of the PAVA and NACT inversion approaches.

**Figure 20** shows maps of shear-velocity anomalies at depths of 600 and 800 km, spanning the 650 km discontinuity for the three models discussed above; it also shows the power spectra for those models at both depths. All models show strong degree-2 in the transition zone and significantly weaker, whiter spectrum in the lower mantle. This is similar to the result obtained by Gu *et al.* (2001), which pointed out the abrupt change in the pattern of lateral heterogeneity above and below 650 km discontinuity.

**Figure 21** compares the power spectra of the three models as a function of depth. The increase in degree-2 power is limited to the transition zone and does not extend either above or below; this indicates that the transition zone is a boundary layer (Dziewonski *et al.*, 2006), and the flux between the upper and lower mantle is likely to be significantly impeded. The similarity of the models indicates robustness of the results and that the differences caused by using different theories and data sets are not sufficient to overwhelm convergence of the modeling effort. Favorable comparisons of features in models obtained by different research groups is probably the most practical approach to assessing credibility of tomographic models or their specific features.

The question of using ‘better theory’ has been brought to focus by the work of Montelli *et al.* (2004a, 2004b) who adopted the ‘banana-doughnut’ (finite-frequency) algorithm (Dahlen *et al.*, 2000) to inversion of teleseismic P-wave data set for a 3-D model of the mantle. These authors suggested that it was the application of this theory which allowed them to map plumes in the mantle. However, comparison of the velocity anomaly maps of models obtained using both ray theory and finite-frequency kernels reveals that maps are essentially identical, except for a constant scaling factor of 1.13 (van der Hilst and de Hoop, 2005). A pair of maps (from figure 8 of Montelli *et al.*, 2004b) at a depth of

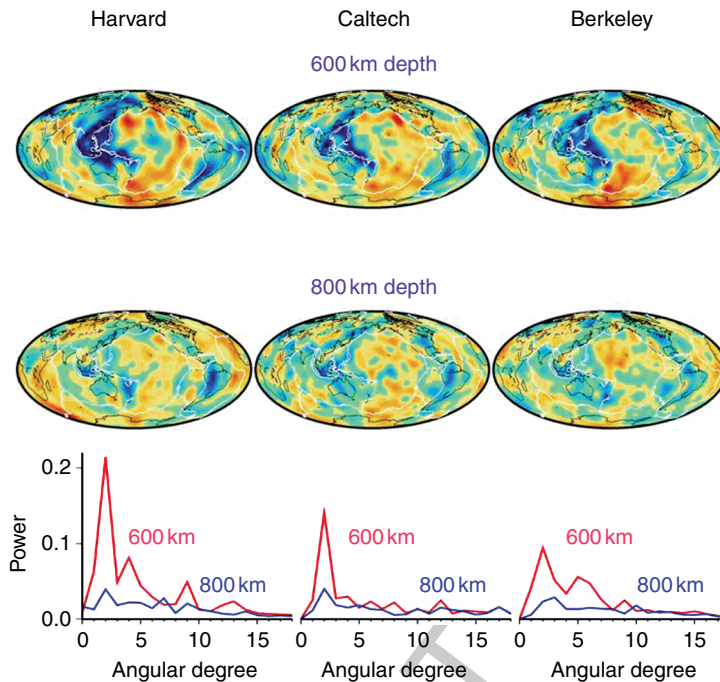


**Figure 20** Maps from the three models that use data sets (overtones/waveforms) that control the structure in the transition zone (Ritsema *et al.*, 1999; Panning and Romanowicz, 2006; Kustowski *et al.*, 2006). The difference between the maps at 600 and 800 km depth is large both in the space and wave-number domains, leading to the conclusion that the transition zone represents a boundary layer that may impede the flow between the upper and lower mantle. The strong degree-2 signal in the transition zone correlates with the location of subduction in the western Pacific and to a lesser extent, under South America.

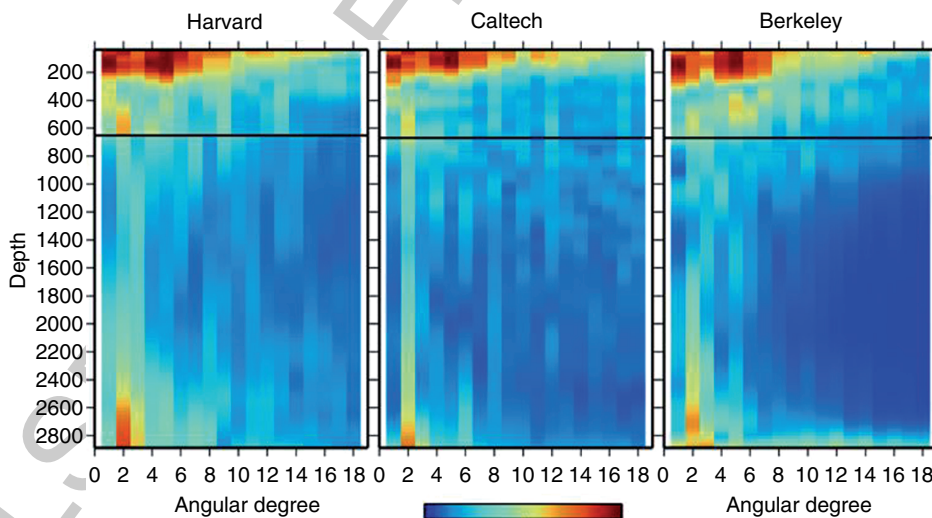


**Figure 21** Comparison of the power spectra as a function of depth for the three models discussed in **Figure 20**. All models show a surface boundary layer dominated by degree 5; a boundary layer near the core–mantle boundary, dominated by degrees 2 and 3; and an additional boundary layer – the third most prominent feature in the Earth models – in the transition zone.

2750 km is shown in **Figure 22**. All the same features are present in both maps (including the alleged plumes); only a slight scaling effect can be seen,

with amplitudes being higher in the ‘finite-frequency’ map. One way to interpret this picture is that, in this particular case, the ‘ray theory’ and ‘finite-frequency’

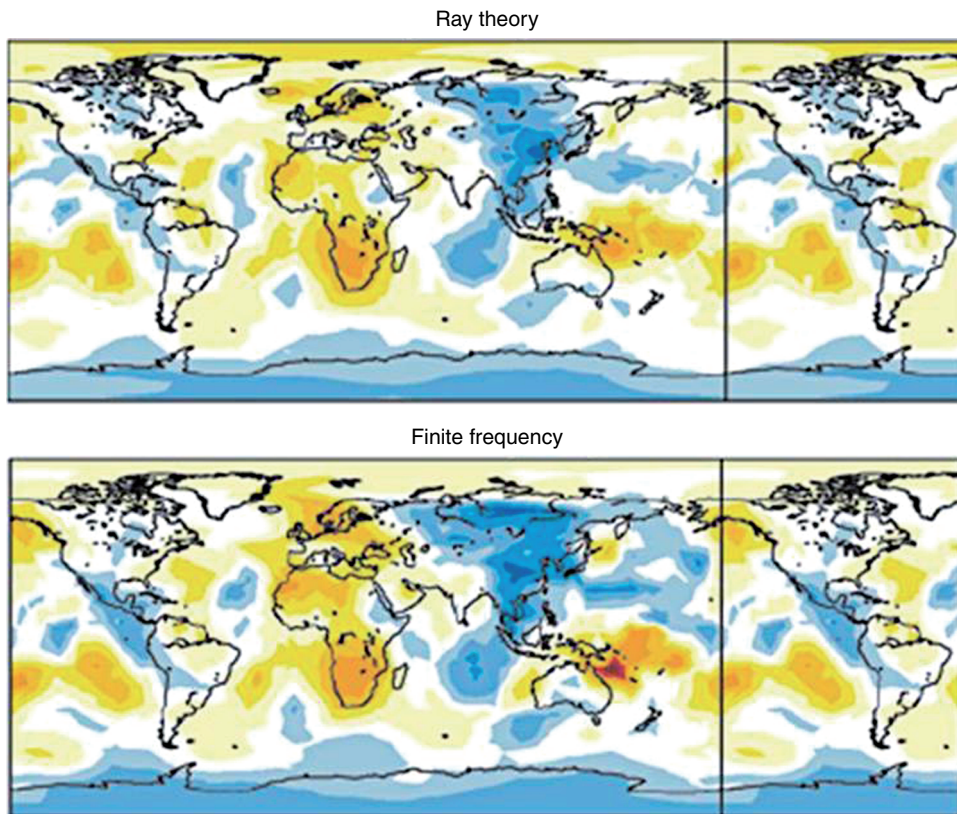


**Figure 22** Comparison of two maps of P-velocity anomalies at 2750 km depth from the models of Montelli *et al.* (2004b). It is very difficult to identify a feature that is different in the ‘ray theory’ model (left) and ‘finite frequency’ model (right); there is a constant scaling factor between the two results (van der Hilst and de Hoop, 2005), which does not change the conclusion that the difference between the two models does not have a geophysical significance. Modified from Montelli R, Nolet G, Dahlen F, Masters G, Engdahl E, and Hung SH (2004b) Finite-frequency tomography reveals a variety of plumes in the mantle. *Science* 303: 338–343.

approaches lead to nearly identical results. The important point is that this negates the implication of the papers by Montelli *et al.* that results obtained using ray theory cannot be trusted, possibly invalidating much of tomographic research during the previous quarter of the century.

A number of papers have been published on the question of using first-order scattering (Born) theory in inversion of seismic data (cf. Boschi *et al.*, 2006); in general, conclusions were that the difference was not substantial and in some cases Born theory gave even worse results. It should be realized that the way that ray theory is applied in practice, with finite area or volume parametrization and matrix conditioning (smoothness, in particular), it really does not involve an infinitely thin ray, but rather a finite area or volume, which will also be sampled by nearby rays, thus introducing smoothing of the structure. This is illustrated in **Figure 23** (from Nettles, 2005)

comparing the best representation of a ‘ray’ in the local basis expansion using 362 spherical splines; these ‘fat rays’ are compared with the ‘influence zone’ computed for 40-s and 150-s Love waves using the method developed by Yoshizawa and Kennett (2002); the ‘fat rays’ are broader than the ‘influence zones’, indicating that, from the point of finite-frequency theory, spherical splines with a smaller radius could be adopted to resolve finer details of the structure. It may be that, when the wavelength of a seismic wave and the distance between the source and receiver are comparable, the finite-frequency approach can be important. Clearly, improvements in theory are needed; development of accurate numerical methods for the computation of ‘exact’ synthetic seismograms for 3-D Earth models (*see* 00006) already provides the means for comparison of various approximations used in inverse problems.

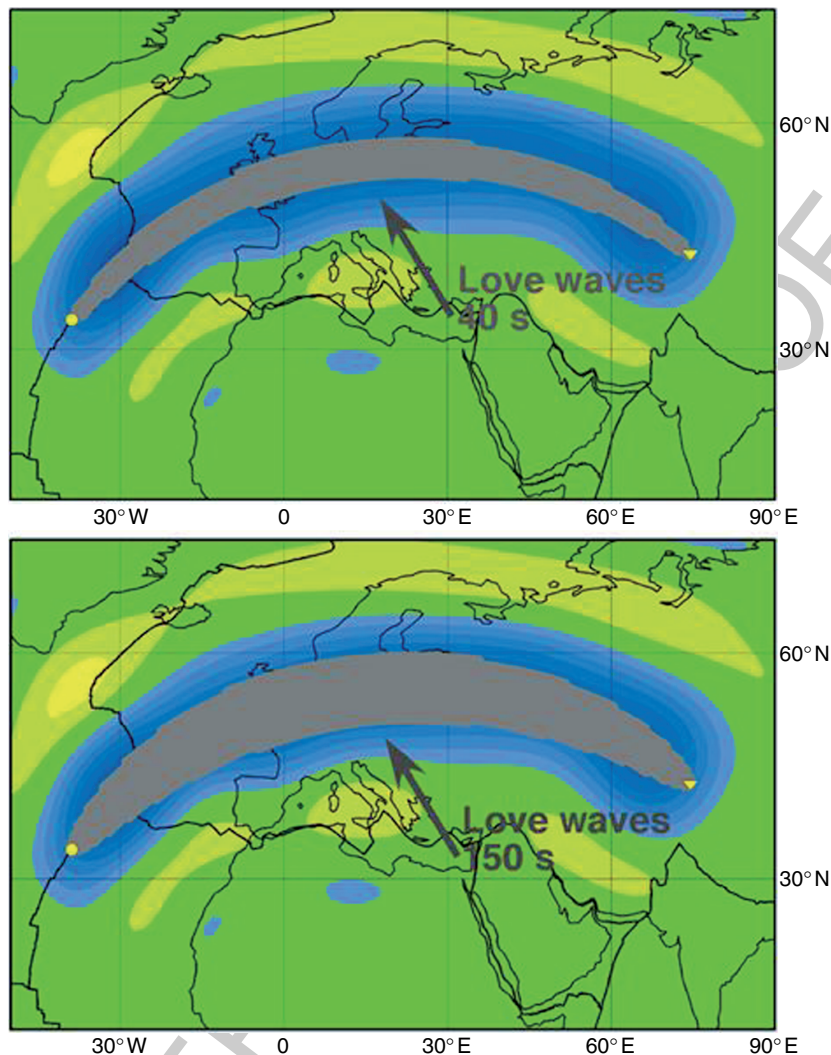


**Figure 23** Basis function (spherical caps) expansion of a minor-arc raypath, which illustrates that the ‘infinitely thin’ rays become quite substantial when parametrized, in this case, using 362 caps (blue area). The ‘area of influence’ of Yoshizawa and Kennett (2002, shown in gray) for 40-s (top) and 150-s (bottom) Love waves is shown for comparison. From Nettles M (2005) *Anisotropic velocity structure of the mantle beneath North America*. PhD Thesis, Harvard University.

## References

- b0005** Adams RD, *et al.* (2002) International seismology. In: Lee WHK, Kanamori H, Jennings PC, and Kisslinger C (eds.) *International Handbook of Earthquake and Engineering Seismology Part A*, pp. 29–37. San Diego, CA: Academic Press.
- b0010** Agnew DC, *et al.* (2002) History of seismology. In: Lee WHK, Kanamori H, Jennings PC, and Kisslinger C (eds.) *International Handbook of Earthquake and Engineering Seismology*, pp. 3–12. San Diego, CA: Academic Press.
- b0015** Agnew D, Berger J, Buland R, Farrell W, and Gilbert F (1976) International deployment of accelerometers: A network for very long period seismology. *EOS, Transactions of American Geophysical Union* 57: 180–188.
- b0020** Agnew DC, Berger J, Farrell WE, Gilbert JF, Masters G, and Miller D (1986) Project IDA; a decade in review. *EOS, Transactions of American Geophysical Union* 67: 203–212.
- Aki K, Christofferson A, and Husebye E (1977) Determination of the three-dimensional structure of the lithosphere. *Journal of Geophysical Research* 82: 277–296.
- Alsop LE, Sutton GH, and Ewing M (1961) Free oscillations of the Earth observed on strain and pendulum seismographs. *Journal of Geophysical Research* 66: 631–641.
- Alterman Z, Jarosch H, and Pekeris CL (1959) Oscillations of the Earth. *Proceedings of the Royal Society of London, Series A* 259: 80–95.
- Anderson DL and Hart RS (1978) Q of the Earth. *Journal of Geophysical Research* 83: 5869–5882.
- Anderson DL and Archambeau CB (1964) The anelasticity of the Earth. *Journal of Geophysical Research* 69: 2071–2084.

- b0050** Backus GE and Gilbert F (1961) The rotational splitting of free oscillations of the Earth. *Proceedings of the National Academy of Sciences of the United States of America* 47: 362–371.
- b0055** Backus GE and Gilbert F (1967) Numerical applications of formalism for geophysical inverse problems. *Geophysical Journal of the Royal Astronomical Society* 13: 247–276.
- b0060** Backus GE and Gilbert F (1968) The resolving power of gross Earth data. *Geophysical Journal of the Royal Astronomical Society* 16: 169–205.
- b0065** Backus GE and Gilbert F (1970) Uniqueness in the inversion of gross Earth data. *Philosophical Transactions of the Royal Society of London, Series A* 266: 169–205.
- b0070** Benndorf H (1905) Über die Art der Fortpflanzung der Erdbebenwellen im Erdinneren. 1. Mitteilung. Sitzungsberichte der Kaiserlichen Akademie in Wien. *Mathematisch-Naturwissenschaftliche Klasse 114, Mitteilungen der Erdbebenkommission*, Neue Folge 29, 1–42.
- b0075** Benndorf H (1906) Über die Art der Fortpflanzung der Erdbebenwellen im Erdinneren. 2. Mitteilung. Sitzungsberichte der Kaiserlichen Akademie in Wien. *Mathematisch-Naturwissenschaftliche Klasse 115, Mitteilungen der Erdbebenkommission*, Neue Folge 31, 1–24.
- b0080** Berkner LV, et al. (1959) *Report of the Panel on Seismic Improvement. The Need for Fundamental Research in Seismology*, 212pp. Washington, DC: Department of State.
- AU20**
- b0085** Boschi L and Dziewonski AM (1999) 'High' and 'low' resolution images of the Earth's mantle – Implications of different approaches to tomographic modeling. *Journal of Geophysical Research* 104: 25567–25594.
- b0090** Boschi L, Becker TW, Soldati G, and Dziewonski AM (2006) On the relevance of Born theory in global seismic tomography. *Geophysical Research Letters* 33: L06302 (doi:10.1029/2005GL025063).
- b0095** Cooley JW and Tukey JW (1965) An algorithm for machine computation of complex Fourier series. *Mathematics of Computation* 19: 297–301.
- b0100** Dahlen F, Hung S-H, and Nolet G (2000) Fréchet kernels for finite-frequency traveltimes – I. Theory. *Geophysical Journal International* 141: 157–174.
- b0105** Dziewonski AM (1984) Mapping the lower mantle: Determination of lateral heterogeneity in  $SP\delta$ -velocity up to degree and order 66. *Journal of Geophysical Research* 89: 5929–5952.
- b0110** Dziewonski AM and Anderson DL (1981) Preliminary Earth model (PREM) *Physics of the Earth and Planetary Interiors* 25: 297–356.
- b0115** Dziewonski AM, Chou T-A, and Woodhouse JH (1981) Determination of earthquake source parameters from waveform data for studies of global and regional seismicity. *Journal of Geophysical Research* 86: 2825–2852.
- b0120** Dziewonski AM and Gilbert F (1971) Solidity of the inner core of the Earth inferred from normal mode observations. *Nature* 234: 465–466.
- b0125** Dziewonski AM and Gilbert F (1972) Observations of normal modes from 84 recordings of the Alaskan earthquake of 28 March 1964. *Geophysical Journal of Royal Astronomical Society* 27: 393–446.
- b0130** Dziewonski AM and Gilbert F (1973) Observations of normal modes from 84 recordings of the Alaskan earthquake of 28 March 1964, Part II: Spheroidal overtones from 285–100 seconds. *Geophysical Journal of the Royal Astronomical Society* 35: 401–437.
- b0135** Dziewonski AM and Gilbert F (1974) Temporal variation of the seismic moment tensor and the evidence of precursive compression for two deep earthquakes. *Nature* 247: 185–188.
- b0140** Dziewonski AM and Haddon RAW (1974) The radius of the core–mantle boundary inferred from travel time and free oscillation data: A critical review. *Physics of the Earth and Planetary Interiors* 9: 28–35.
- Dziewonski AM, Hager BH, and O'Connell RJ (1977) Large scale heterogeneities in the lower mantle. *Journal of Geophysical Research* 82: 239–255. **b0145**
- Dziewonski AM and Hales AL (1972) Numerical analysis of dispersed seismic waves. In: Adler B, Fernbach S, and Bolt BA (eds.) *Methods in Computational Physics*, vol. 11, pp. 39–85. New York: Academic Press. **b0150**
- Dziewonski AM, Hales AL, and Lapwood ER (1975) Parametrically simple Earth models consistent with geophysical data. *Physics of the Earth and Planetary Interiors* 10: 12–48. **b0155**
- Dziewonski AM and Woodward RL (1992) Acoustic imaging at the planetary scale. In: Ermer H and Harjes H-P (eds.) *Acoustical Imaging*, vol. 19, pp. 785–797. New York: Plenum Press. **b0160**
- Ekström G, Tromp J, and Larson EW (1997) Measurements and models of global surface wave propagation. *Journal of Geophysical Research* 102: 8137–8157. **b0165**
- Ekström G, Dziewonski AM, Maternovskaya NN, and Nettles M (2005) Global seismicity of 2003: Centroid-moment-tensor solutions for 1087 earthquakes. *Physics of the Earth and Planetary Interiors* 148: 327–351. **b0170**
- Ewing M, Jardetzky WS, and Press F (1957) *Elastic Waves in Layered Media*. New York: McGraw-Hill. **b0175**
- Ewing M and Press F (1954) An investigation of mantle Rayleigh waves. *Bulletin of the Seismological Society of America* 44: 127–148. **b0180**
- Fuchs K and Müller G (1971) Computation of synthetic seismograms and comparison with observations. *Geophysical Journal of the Royal Astronomical Society* 23: 417–433. **b0185**
- Galitzin (also Golicyn) BB (1914) *Vorlesungen über Seismometrie*, deutsche Bearbeitung unter Mitwirkung von Clara Reinfeldt, herausgegeben von Oskar Hecker, vol. VIII, 538pp. Berlin: Verlag Teubner. **b0190**
- Geiger L (1910) Herdbestimmung bei Erdbeben aus den Ankunftszeiten. Nachrichten von der Königlichen Gesellschaft der Wissenschaften zu Göttingen. *Mathematisch-physikalische Klasse* 331–349. (Translated into English by Peebles FWL, Anthony H, Corey SJ) **b0195**
- Geiger L (1912) Probability method for the determination of earthquake epicenters from the arrival time only. *Bulletin of St. Louis University* 8: 60–71. **b0200**
- Gilbert F and Dziewonski AM (1975) An application of normal mode theory to the retrieval of structural parameters and source mechanisms from seismic spectra. *Philosophical Transactions of the Royal Society of London, Series A* 278: 187–269. **b0205**
- Green RWE and Hales AL (1968) Travel times of P waves to 30 degrees in central United States and upper mantle structure. *Bulletin of the Seismological Society of America* 58: 267–289. **b0210**
- Gu YJ, Dziewonski AM, and Ekström G (2003) Simultaneous inversion for mantle shear velocity and topography of transition zone discontinuities. *Geophysical Journal International* 154: 559–583. **b0215**
- Gu JY, Dziewonski AM, Su W-J, and Ekström G (2001) Shear velocity model of the mantle and discontinuities in the pattern of lateral heterogeneities. *Journal of Geophysical Research* 106: 11169–11199. **b0220**
- Gutenberg B (1913) Über die Konstitution des Erdinneren, erschlossen aus Erdbebenbeobachtungen. *Physikalische Zeitschrift* 14: 1217–1218. **b0225**
- Gutenberg B and Richter CF (1934) On seismic waves (first paper). *Gerlands Beiträge Zur Geophysik* 43: 56–133. **b0230**
- Gutenberg B and Richter CF (1936) On seismic waves (third paper). *Gerlands Beiträge Zur Geophysik* 47: 73–131. **b0235**
- Hales AL, Lapwood ER, and Dziewonski AM (1974) Parameterization of a spherically symmetrical Earth model **b0240**

- with special references to the upper mantle. *Physics of the Earth and Planetary Interiors* 9: 9–12.
- b0245** Harjes H-P and Seidl D (1978) Digital recording and analysis of broad-band seismic data at the Gräfenberg (GRF) array. *Journal of Geophysics* 44: 511–523.
- b0250** Haskell NA (1953) The dispersion of surface waves on multilayered media. *Bulletin of the Seismological Society of America* 43: 17–43.
- b0255** Herglotz G (1907) Über das Benndorfsche Problem der Fortpflanzungsgeschwindigkeit der Erdbebenwellen. *Physikalische Zeitschrift* 8: 145–147.
- b0260** Inoue H, Fukao Y, Tanabe K, and Ogata Y (1990) Whole mantle P-wave travel time tomography. *Physics of the Earth and Planetary Interiors* 59: 294–328.
- b0265** Jeffreys H (1926) The rigidity of the Earth's central core. *Monthly Notices of the Royal Astronomical Society, Geophysical Supplement* 1: 371–383.
- b0270** Jeffreys H and Bullen KE (1940) *Seismological Tables*, 50pp. London: British Association for the Advancement of Science.
- b0275** Jobert N (1956) Évaluation de la période d'oscillation d'une sphere hétérogène, par application du principe de Rayleigh. *Comptes Rendus De L Academie Des Sciences, Paris* 243: 1230–1232.
- b0280** Jobert N (1957) Sur la période propre des oscillations sphéroïdales de la Terre. *Comptes Rendus De L Academie Des Sciences, Paris* 244: 242–258.
- b0285** Jobert N (1961) Calcul approché de la période des oscillations sphéroïdales de la Terre. *Geophysical Journal of the Royal Astronomical Society* 4: 242–258.
- b0290** Jordan TH (1978) A procedure for estimating lateral variations from low-frequency eigenspectra data. *Geophysical Journal of the Royal Astronomical Society* 52: 441–455.
- b0295** Jordan TH and Anderson DL (1974) Earth structure from free oscillations and travel times. *Geophysical Journal of the Royal Astronomical Society* 36: 411–459.
- b0300** Julian BR and Sengupta MK (1973) Seismic travel time evidence for lateral inhomogeneity in the deep mantle. *Nature* 242: 443–447.
- b0305** Kennett BLN, Engdahl ER, and Buland R (1995) Constraints on seismic velocities in the Earth from traveltimes. *Geophysical Journal International* 122: 108–124.
- b0310** Knott CG (1899) Reflection and refraction of elastic waves, with seismological applications. *The London, Edinburgh, and Dublin Philosophical Magazine and Journal of Science, Series 5* 48: 64–97/ 567–569.
- b0315** Landisman M, Sato Y, and Nafe JE (1965) Free vibrations of the Earth and the properties of its deep interior regions: Part 1. Density. *Geophysical Journal of the Royal Astronomical Society* 9: 439–502.
- b0320** Lehmann I (1936) P'. *Publ. Bureau Cent. Séism. Inter., Série A, Trav. Scient* 14: 87–115.
- b0325** Li XD and Tanimoto T (1993) Waveforms of long-period body waves in a slightly aspherical Earth model. *Geophysical Journal International* 112: 92–102.
- b0330** Li XD and Romanowicz B (1995) Comparison of global waveform inversions with and without considering cross branch coupling. *Geophysical Journal International* 121: 695–709.
- b0335** Li X-D and Romanowicz B (1996) Global mantle shear velocity model developed using nonlinear asymptotic coupling theory. *Journal of Geophysical Research* 101: 22245–22272.
- b0340** Liu H-P, Anderson DL, and Kanamori H (1976) Velocity dispersion due to anelasticity: Implications for seismology and mantle composition. *Geophysical Journal of the Royal Astronomical Society* 47: 41–58.
- b0345** Love AEH (1911) *Some Problems of Geodynamics*. Cambridge: Cambridge University Press.
- b0350** Masters G, Jordan TH, Silver PG, and Gilbert F (1982) Aspherical earth structure from fundamental spheroidal mode data. *Nature* 298: 609–613.
- Mégnin C and Romanowicz B (1999) The effects of the theoretical formalism and data selection on mantle models derived from waveform tomography. *Geophysical Journal International* 138: 366–380.
- b0355**
- Mendiguren J (1973) Identification of free oscillation spectral peaks for 1970 July 31, Colombian deep shock using the excitation criterion. *Geophysical Journal of the Royal Astronomical Society* 33: 281–321.
- b0360**
- Mohorovičić A (1910) Potres od 8. X 1909. God. Izvješće Zag. met. Ops. Zag. 1909, Zagreb (Das Beben vom 8. X 1909. *Jahrbuch des meteorologischen Observatoriums in Zagreb für das Jahr 1909*), 9, Part 4, 1–63.
- b0365**
- Montelli R, Nolet G, Dahlen F, Masters G, Engdahl E, and Hung SH (2004a) Global P and PP travel time tomography: Rays vs. waves. *Geophysical Journal International* 158: 637–654.
- b0370**
- Montelli R, Nolet G, Dahlen F, Masters G, Engdahl E, and Hung SH (2004b) Finite-frequency tomography reveals a variety of plumes in the mantle. *Science* 303: 338–343.
- b0375**
- Ness NF, Harrison JC, and Slichter LB (1961) Observations of the free oscillations of the Earth. *Journal of Geophysical Research* 66: 621–629.
- b0380**
- Nettles M (2005) *Anisotropic velocity structure of the mantle beneath North America*. PhD Thesis, Harvard University.
- b0385**
- Panning M and Romanowicz B (2006) A three dimensional radially anisotropic model of shear velocity in the whole mantle. *Geophysical Journal International* 167: 361–379.
- b0390**
- Pekeris CL, Alterman Z, and Jarosch H (1961a) Comparison of theoretical with observed values of the periods of the free oscillations of the Earth. *Proceedings of the National Academy of Sciences of the United States of America* 47: 91–98.
- b0395**
- Pekeris CL, Alterman Z, and Jarosch H (1961b) Rotational multiplets in the spectrum of the Earth. *Physical Review* 122: 1692–1700.
- b0400**
- Pekeris CL and Jarosch H (1958) The free oscillations of the Earth. In: Benioff H, Ewing M, Howell jun BF, and Press K (eds.) *Contributions in Geophysics in Honor of Beno Gutenberg et al*, pp. 171–192. New York: Pergamon.
- b0405**
- Peterson J, Butler HM, Holcomb LT, and Hutt C (1976) The seismic research observatory. *Bulletin of the Seismological Society of America* 66: 2049–2068.
- b0410**
- Poupinet G, Frechet J, and Thouvenot F (1989) Portable short period vertical seismic stations transmitting via telephone or satellite. In: Cassinis R and Nolet G (eds.) *Digital Seismology and Fine Modelling of the Lithosphere*, pp. 9–26. London: Plenum.
- b0415**
- Press F (1956) Determination of crustal structure from phase velocity of Rayleigh waves – Part I. Southern California. *Bulletin of Geological Society of America* 67: 1647–1658.
- b0420**
- Rayleigh JWS (1885) On waves propagated along plane surface of an elastic solid. *Proceedings of the London Mathematical Society* 17: 4–11.
- b0425**
- Rebeur-Paschwitz E v (1889) The earthquake of Tokyo, April 18, 1889. *Nature* 40: 294–295.
- b0430**
- Ritsema J, van Heijst HH, and Woodhouse JH (1999) Complex shear wave velocity structure imaged beneath Africa and Iceland. *Science* 286: 1925–1928.
- b0435**
- Ritsema J, van Heijst HJ, and Woodhouse JH (2004) Global transition zone tomography. *Journal of Geophysical Research* 109: B02302 (doi:10.1029/2003JB002610).
- b0440**
- Romanowicz B (1979) Seismic structure of the upper mantle beneath the United States by three-dimensional inversion of body wave arrival times. *Geophysical Journal of the Royal Astronomical Society* 57: 479–506.
- b0445**
- Romanowicz B (1991) Seismic tomography of the Earth's mantle. *Annual Review of Earth and Planetary Science* 19: 77–99.
- b0450**
- Romanowicz B (2003) Global mantle tomography: Progress status in the last 10 years. *Annual Review of Geophysics and Space Physics* 31: 303–328.
- b0455**

- b0460 Romanowicz BA, Cara M, Fels JF, and Roulard D (1984) Geoscope: A French initiative in long-period three-component seismic networks. *EOS Transactions of American Geophysical Union* 65: 753–754.
- b0465 Romanowicz BA and Dziewonski AM (1986) Towards a federation of broadband seismic networks. *EOS Transactions of American Geophysical Union* 67: 541–542.
- b0470 Russakoff D, Ekström G, and Tromp J (1998) A new analysis of the great 1970 Colombia earthquake and its isotropic component. *Journal of Geophysical Research* 102: 20423–20434.
- b0475 Sailor RV and Dziewonski AM (1978) Observations and interpretation of attenuation of normal modes. *Geophysical Journal of the Royal Astronomical Society* 53: 559–581.
- b0480 Souriau A and Souriau M (1983) Test of tectonic models by great-circle Rayleigh waves. *Geophysical Journal of the Royal Astronomical Society* 73: 533–551.
- b0485 Steim JM (1986) *The very-broad-band seismograph*, 184pp. Doctoral Thesis, Department of Geological Sciences, Harvard University, Cambridge, MA.
- b0490 Stoneley R (1928) A Rayleigh wave problem. *Proceedings of the Leeds Philosophical and Literary Society (Science Section)* 1: 217–225.
- b0495 Su W-J and Dziewonski AM (1991) Predominance of long-wavelength heterogeneity in the mantle. *Nature* 352: 121–126.
- b0500 Su W-J and Dziewonski AM (1992) On the scale of mantle heterogeneity. *Physics of the Earth and Planetary Interiors* 74: 29–54.
- b0505 Takeyuchi H (1959) Torsional oscillations of the Earth and some related problems. *Geophysical Journal of the Royal Astronomical Society* 2: 89–100.
- b0510 Thomson ST (1950) Transmission of elastic waves through a stratified solid medium. *Journal of Applied Physics* 21: 89–93.
- b0515 Toksöz MN and Anderson DL (1966) Phase velocities of long-period surface waves and structure of the upper mantle. *Journal of Geophysical Research* 71: 1649–1658.
- b0520 Udias A and Stauder W (2002) The Jesuit contribution to seismology. In: Lee WHK, Kanamori H, Jennings PC, and Kisslinger C (eds.) *International Handbook of Earthquake and Engineering Seismology et al*, pp. 19–27. San Diego, CA: Academic Press.
- b0525 van der Hilst RD and deHoop MV (2005) Banana-doughnut kernels and mantle tomography. *Geophysical Journal International* 163: 956–961.
- b0530 van der Hilst R, Kennett B, Christie D, and Grant J (1994) Project Skippy explores the lithosphere and upper mantle below Australia. *EOS Transactions of the American Geophysical Union* 75 177/ 180–181.
- van Heijst HJ and Woodhouse JH (1997) Measuring surface-wave overtone phase velocities using a mode-branch stripping technique. *Geophysical Journal International* 131: 209–230. b0535
- Wiechert E (1907) Über Erdbebenwellen. Theoretisches über die Ausbreitung der Erdbebenwellen. *Nachrichten von der Königlichen Gesellschaft der Wissenschaften zu Göttingen, Mathematisch-physikalische Klasse* 413–529. b0540
- Wielandt E and Streckeisen G (1982) The leaf-spring seismometer: Design and performance. *Bulletin of the Seismological Society of America* 72: 2349–2367. b0545
- Wielandt E and Steim JM (1986) A digital very-broad-band seismograph. *Annales Geophysicae* 4: 227–232. b0550
- Woodhouse JH (1980) The coupling and attenuation of nearly resonant multiplets in the Earth's free oscillation spectrum. *Geophysical Journal of the Royal Astronomical Society* 61: 261–283. b0555
- Woodhouse JH and Dahlen FA (1978) The effect of a general aspherical perturbation on the free oscillations of the Earth. *Geophysical Journal of the Royal Astronomical Society* 53: 335–354. b0560
- Woodhouse JH and Dziewonski AM (1984) Mapping the upper mantle: Three dimensional modeling of earth structure by inversion of seismic waveforms. *Journal of Geophysical Research* 89: 5953–5986. b0565
- Woodhouse J and Dziewonski A (1986) Three dimensional mantle models based on mantle wave and long period body wave data. *EOS Transactions of the American Geophysical Union* 67: 307. b0570
- Woodhouse JH and Dziewonski AM (1989) Seismic modelling of the Earth's large-scale three dimensional structure. *Philosophical Transactions of the Royal Society of London, Series A* 328: 291–308. b0575
- Woodward RL, Dziewonski AM, and Peltier WR (1994) Comparisons of seismic heterogeneity models and convective flow calculations. *Geophysical Research Letters* 21: 325–328. b0580
- Zöppritz K (1907) Über Erdbebenwellen. II: Laufzeitkurven. *Nachrichten von der Königlichen Gesellschaft der Wissenschaften zu Göttingen, Mathematisch-physikalische Klasse* 529–549. b0585

## Relevant Website

<http://www.globalcmt.org>– Global CMT Web Page.

**Author's Contact Information****[AU1] A. M. Dziewonski**

Department of Geological Sciences  
Harvard University  
20, Oxford Street  
Cambridge  
MA 02138  
USA

**B. A. Romanowicz**

Berkeley Seismological Laboratory  
University of California at Berkeley  
207 McCone Hall  
Berkeley  
CA 94720-4760  
USA

ELSEVIER FIRST PROOF